7-2015

Swelling-Etching Characterization of Copper (I) Oxide - PDMS for the Development of Micro/Nano - Particles Composite MEMS Corrosion Sensor

Abdoul Kader Maiga
University of Arkansas, Fayetteville

Swelling-Etching Characterization of Copper (I) Oxide – PDMS for the Development of Micro/Nano – Particles Composite MEMS Corrosion Sensor

Swelling-Etching Characterization of Copper (I) Oxide – PDMS for the Development of Micro/Nano – Particles Composite MEMS Corrosion Sensor

A thesis submitted in partial fulfillment
of the requirements for the degree of
Master of Science in Mechanical Engineering

by

Abdoul Kader Maiga
University of Arkansas
Bachelor of Science in Mechanical Engineering, 2012

July 2015
University of Arkansas

This thesis is approved for recommendation to the Graduate Council.

Dr. Po-Hao Adam Huang
Thesis Director

Dr. David C. Jensen
Committee Member

Dr. Uchechukwu C. Wejinya
Committee Member

Abstract

The primary objective for this thesis is to contribute to the understanding of the oxide removal process for a corrosion sensing device. The goal for designing such a device is for monitoring corrosion on metallic structures. The sensing material (6.35mm x 1mm discs) of the device is composed of copper (I) oxide particles mixed in some polydimethylsiloxane (PDMS). The PDMS, "housing," is meant for controlling the oxidation rate through the sensing material. A solvent was used to facilitate the etchant diffusion through the PDMS matrix. Toluene and acetic acid were the ideal solvent and etchant, respectively, for carrying out the oxide removal process. [1] The experimental setup used a Microsoft® LifeCam to measure the expansion of the sensing material submitted to the oxide removal process. LabVIEW™ and Vision Assistant™ where used to acquire and store the swelling data, which was then analyzed in Matlab®. There were two oxide removal processes adopted in this thesis. The first process consisted of submerging the copper (I) oxide to PDMS composite sample in toluene until it reached its known maximum growth size and then adding the etchant to carry out the oxide removal process. This process proved to be efficient and failure proof. Though the time for reaching maximum growth weighed against the oxide removal time, this process ensured a thorough oxide etching within the sensing material. The second process consisted of premixing the solvent and etchant prior to submerging the copper (I) oxide to PDMS composites. The second process proved to be faster than the first process, since the sample was not initially grown to its maximum size, with an average time constant (maximum swelling and supposedly complete oxide removal time) differed by about half the average time constant of the first process. Two different growth instances with two different time constants were observed on the graphs of the second process. These instances could be caused by the removal of the oxide which had previously stiffened the PDMS structure prohibiting the solvent from reaching

certain areas of the PDMS's matrix. Once the oxide removed, those areas were exposed permitting the solvent to have access thus causing a second distinct growth instance for the same copper (I) oxide composite sample.

Acknowledgement

I would like to thank my parents for supporting me for all of these years and for never giving up on me. I would like to acknowledge my friends and all the families, here in North West Arkansas that so kindly took me in and made me feel at home here in Arkansas. I would also like to acknowledge my advisor Dr. Adam Huang for the support and guidance throughout my undergraduate honors research project and thesis and graduate Master's research and thesis. I appreciate the understanding and support from the Mechanical Engineering staff, for granting me with a Teaching Assistantship and trusting me to complete my Masters work on time, and faculty, for priceless advices.

Contents

Table of Figures:

List of Tables

Chapter 1. Introduction

1. Research Objective

The hypothesis for this experimental research is that the de-oxidization of copper (I) oxide particles mixed into an inert polymer, PDMS – polydimethylsiloxane, can be achieved by, first, swelling the sensing material then using an etchant to remove the oxide from the copper particles, and second, by premixing both solvent and etchant prior to adding the sensing material in the solution for de-oxidization. This thesis is characterizing the sensing material proposed for the corrosion monitoring device. The **goal** is to fabricate a device that will effectively measure the material (copper) degradation rate of a structure. Research process summary:

1. Use Labview™, Vision Assistant™, and Matlab® to accurately collect data acquisition.
2. Measure the swelling of copper – PDMS composites in Toluene.
3. Obtain best practice for copper (I) oxide- PDMS composites de-oxidization.

2. Corrosion/Oxidation Monitoring

Corrosion management is essential in every industrial and scientific field that uses corrosive materials. Corrosion, being the unintended attack and degradation of materials, occurs at multiple levels on a structure. It may occur at the micro scale, within the granular boundaries of the material, or simply could occur at the surface of a material. Corrosion stress causes catastrophic failures that cost millions of dollars to businesses and government bodies, but most importantly, human lives. For these reasons, a novel real time corrosion monitoring device, being developed at the University of Arkansas Engineering Research Center (ERC) in the EMNSL will monitor the potential degradation and subsequently prevent structures failures due to corrosion stress. In its simplest

form, corrosion monitoring may be described as acquiring data as a rate of material degradation. There are three known techniques used to monitor the oxidation of metallic structures. They are Offline, Inline, and Real Time monitoring methods.

The **Offline monitoring** method gives an average corrosion rate from a structure or a sample coupon obtained from a structure that is failing or has already failed. This technique is effective when the nature for failure of a structure is sought, but ineffective when the failure is to be prevented. The Silver Bridge collapse in 1987 is an example of a catastrophic structural failure that occurred partially due to corrosion fatigue and stress. [2] The researchers in charge of investigating on the issue used an offline technique to determine the origin of the failure after the failure had occurred. [2] Offline monitoring methods have their applications in many structural analysis techniques but are not ideal for monitoring an ongoing corrosion degradation of a structure in order to prevent its failure.

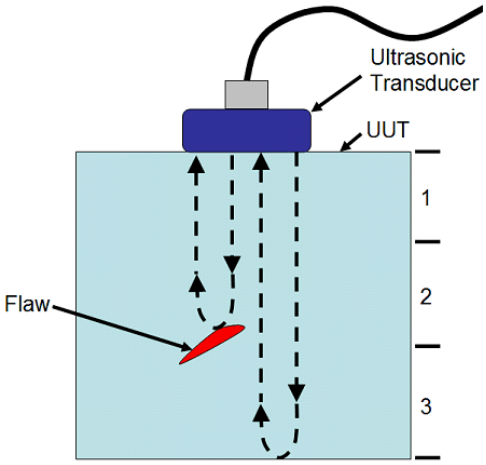

Figure 1: Offline Coupon Scanning using an Acoustic device.

The **Inline monitoring** method uses a probe installed near and/or within the structure to be monitored. It requires that the data obtained be collected intermittently or when the structure has

failed depending on how the probe was installed. This technique also allows one to communicate the data real time using a data logger and a data emitter (wireless or wired emitter). [3]

Figure 2: Example of a probe installed inline on the sample to monitor. [3]

The above image is an example of an inline monitoring installation. The probe is mounted directly on the metallic structure. The idea here is to submit the probe to a corrosion environment similar to that of the structure being monitored. The probe would corrode at the same rate with the structure it is attached to, therefore, by measuring the rate of corrosion of the probe, the corrosion rate of the structure can also be known. The inline monitoring methods does not give a finite monitoring method which is essential for precisely pin pointing areas where failure is likely to occur. This advantage is one driving factor for the novel corrosion monitoring method studied in this thesis.

The **Real Time monitoring** method directly reports information collected thus giving a real time management of the structure's degradation. Real Time corrosion management is a technique for collecting information about a structure while the damage is occurring on the structure. This method finds its application in a multitude of areas. Furnaces, in boilers, operate in such environments that expose their structures to heavy oxidation. Offline and Inline monitoring

techniques require production in plants to slow down or even to stop in order for the data gathered to be collected. [4] That necessary inconvenience costs hundreds of thousands of dollars to the industry sector every year. With Real Time monitoring, downtime can be avoided thus saving industries the down time costs.

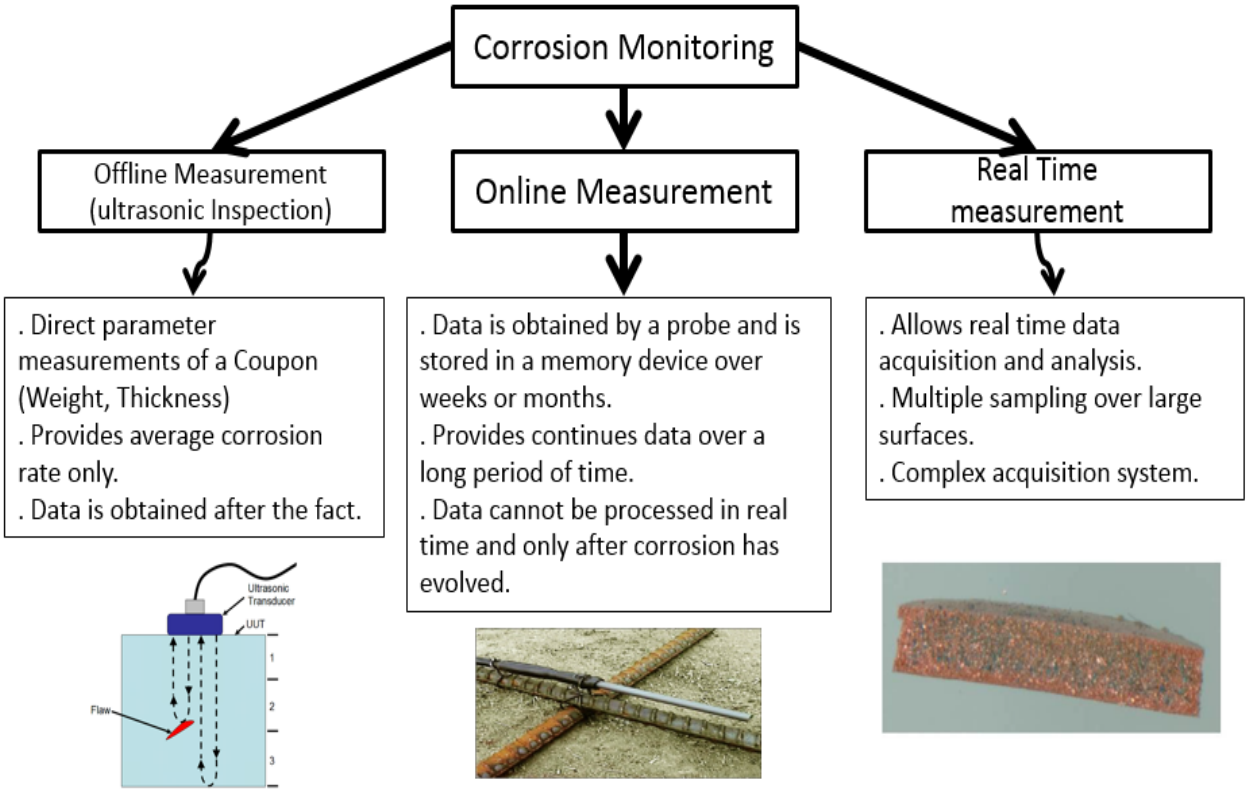

Figure 3: Corrosion sensing techniques with pros and cons.

3. Importance of sensing corrosion defect on apparatus or structures

There is no need for emphasizing the importance for sensing corrosion defects on structures using any known corrosion monitoring method. Corrosion is a naturally occurring phenomenon that has to be considered in the decision for standards and for engineering practices. Oversizing is one common solution for preventing corrosion stress on structure. Oftentimes toxic materials are used in an effort to slowing and prohibiting oxidation from attacking structures. [5] Chemicals such as

Cadmium coatings and Chromium used with steel to make stainless steel, which resist corrosion and de-coloration of the metal, are toxic and potentially carcinogenic if used in large quantities. [5] Many of those methods are rising environmental and health concerns thus making sensing corrosion degradation instead, more valuable. Zinc coating on iron and pure Aluminum layer over Aluminum copper alloys are anodic methods for protecting surfaces form oxidization. Since electrons flow through the protecting layer, the underlying surface is protected from losing or gaining electrons through the electrolytic environment. The potential difference between the environment and the protecting layer is what drives the current through the protecting layer. A cathodic method can also be used to create a current from the protecting layer to the metal in question thus inhabiting any electrochemical reaction between the protecting layer and the metal itself, and the metal itself and the electrolytic environment. Corrosion sensing has been proven necessary because of the many catastrophic failures caused by corrosion stress on metal structures. In the aviation industry alone, several catastrophic failures occur yearly due to corrosion stress. These accidents led to many lives lost and millions of dollars lost in investigations and law suits against the company or individuals to blame. For example, in December 19, 2005, the Chalk's Ocean Airways flight 101 crashed minutes after take-off. The airplane was built in 1926 and had undergone thousands of hours of flight until it crashed. The right wing of the airplane separated in flight causing the airplane to dive to the ground. This structural failure has been blamed on the fact that the plane had exceeded its maximum load during take-off and thus failed. [5] A proposed alternate reason for the failure was old and rusty joints that had not been detected using traditional inspection methods. The wing's rupture could have been prevented if a more advanced and preventive method for inspecting the plane was used. This accident, and many others, that cost thousands of people's life can be avoided in a more preventive structural analysis methods that

uses real time monitoring systems. That is the reason we took on the initiative for developing new technology to address this problem.

4. Types of Corrosions

There exist many types of corrosions, which affects material differently and at different levels. From the surface of materials to the grain boundaries, corrosion can affect most metals and drastically reduce their granular integrity. Corrosion predominantly occurs in high humidity environments where the metal is constantly exposed to corrosive elements such as water and salt. Figure 4 shows three examples of corrosion types which occur at different levels on the material. Figure 4a is an example of inter-granular corrosion which, as its name suggests, is the degradation of the material at a micro scale between the grains boundaries. Figure 4b is an example of dendrites which form on electronic devices, especially on circuit boards connector pads. Figure 4c shows an example of uniform attack on a platform that is near a saline water bed. These three types of corrosion are indeed occurring at different scales that are micrometer scale, Figure 4a, millimeter scale, Figure4b, and centimeter to meter scale.

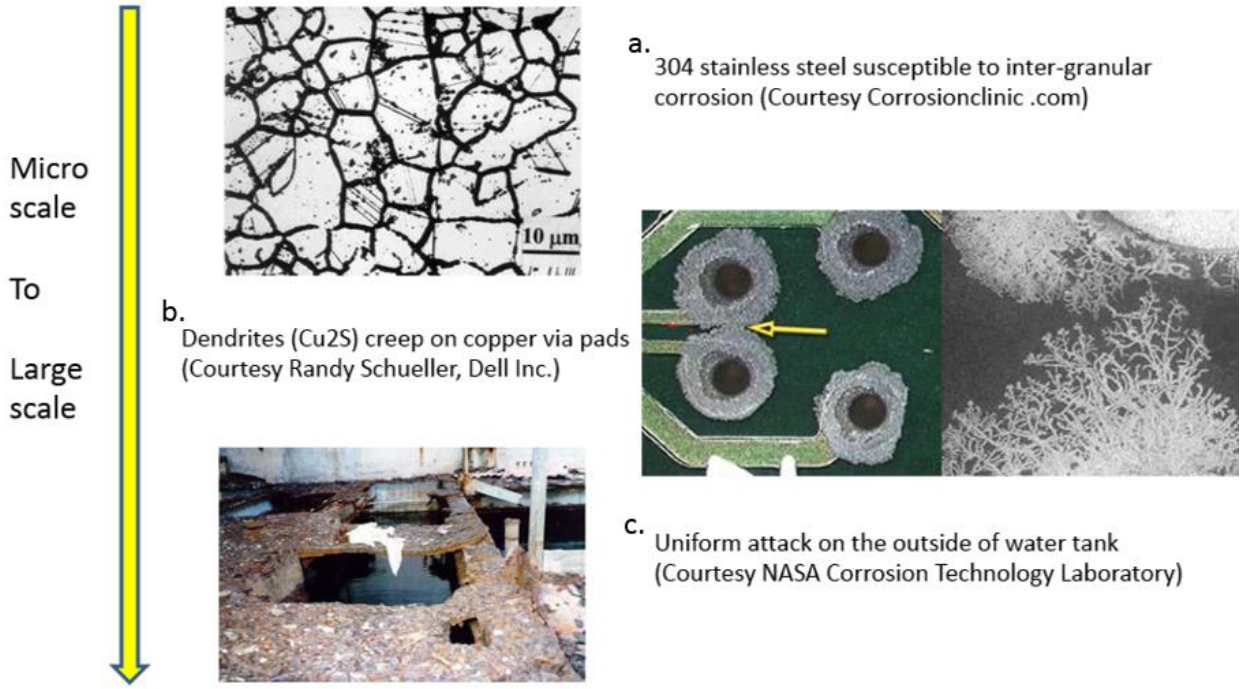

Figure 4: Corrosion types and scales affected. [7]

5. Potential for the sensing technique

The proposed corrosion monitoring technique uses materials for its fabrication that are commonly used in the micro device manufacturing field, especially in MEMS (Micro-Electro-Mechanical Systems) and micro fluidics, therefore making them easily accessible and relatively inexpensive. The fabrication process adopted for fabricating the sensing material ensures that all elements needed are readily found in most micro/Nano fabrication clean rooms. This fact adds to the inexpensive fabrication process of the sensing material thus dramatically increasing the relevance of such a device in the metrology field. It is important to know that any measuring device is as effective as its usability and accessibility. The device must first be usable, that is, the device must perform the measurements as accurately and as precisely as possible and within acceptable timely manners. The cost of the measuring device might make it inaccessible to the interested parties. In these advanced technological days, any device imaginable can eventually be built, but in most

cases the limiting factor is the retail cost. Cost is an underlining factor that surely drive the entire fabrication principle of the corrosion sensing device proposed in this thesis to ensure that once developed, it will be accessible to most interested parties.

6. Preliminary cost analysis

To assist with understanding the low cost aspect of the corrosion sensing device being developed in this thesis, a rough cost analysis was done. Since the development phase of this corrosion device is still premature, several assumptions were made. Though assumptions, the cost associated with fabricating this corrosion monitoring device is well within reasonable ranges and are realistic.

Table 1: Estimated Cost for fabricating a corrosion sensing device.

For One 100 mm Diameter wafer			$ 30.00	each, Borosilicate Glass	
SU-8 Photoresist			$ 10.00	Estimate per waffer	
Copper Particles			$ 10.00	Estimate per waffer	
Polydimethylsiloxane			$ 10.00	Estimate per waffer	
Man hours			$ 250.00	for 10 hours of labor	
Electronics			$ 50.00		
Packaging			$3,600.00	10X the fabrication cost	
Avg Sensor Size	1	mm^2			
Total wafer area	7853.982	mm^2			
Number of Sensors	7853				
Price per Sensor			$ 0.46		

Chapter 2. Sensing Theory

Any conductive material that is available at the market could essentially be ideal candidates for sensing material. The only requirement is that the type of metal it is attached to and monitoring be similar types. The method of using a similar material to monitor the oxidation of a structure is called the direct method. The indirect method consists of measuring the oxidizing factors of the environment within which the structure is in thus predicting which condition promotes oxidization on the structure. It is known that copper conducts electricity. Copper, being under the group 11 in the transition metals group of the periodic table, is one of the best electricity conductors amongst the family of metals, after Silver. In group 11, Silver and gold are the other excellent electric conductors that are abundant, relatively non-toxic, and available in the market. Roentgenium, a rare metal, is the fourth metal in group 11 whose electrical properties are not yet well understood and not available but are assumed to be similar to that of its respective other group elements. Silver's electrical properties are excellent and could have been chosen as the sensing material particle of choice if its unusual excellent electrical conductivity, even with a layer of oxide, could potentially prohibit the sensing principle used in the development of the corrosion sensing device. Gold, commonly used in circuits for its excellent conductivity and resistance to oxidation, was also considered. Due to the fact that gold has a much higher retail cost disqualified it from the metal particle of choice for it could potentially drive the price of the sensing device higher thus making it inaccessible to the interested parties. Out of all four different metals found in group 11 of the transition metals on the periodic table, copper is the ideal candidate, (metal particle of choice) for the development of the corrosion sensing device. Copper is readily available on the market and is affordable enough that it shall not render the developed sensing device inaccessible. Copper conducts electricity sufficiently enough that it can be measured and analyzed for the

corrosion monitoring purpose of the corrosion sensing device. It also corrodes at its surface and, unlike silver, the layer of oxide prohibits electric conductivity from and to the native copper particle, which is the absolute sensing principle for our sensing material. The theory behind the sensing material being developed is that it shall corrode at a similar rate with the metal structure it is attached to. That degradation registered by our sensing material is translated into an electrical signal which is in turn measured via an electronic device. This is a future research project which has been briefly addressed by Pan et al. (2007) in his doctoral dissertation. The signal then analyzed shall give a finite and detailed information on the progression of the oxide over the structure being monitored. This information can then be used to predict the failure of that structure. That in fact is the end goal for developing the proposed corrosion sensing device.

1. Impedance Driven Sensing

The reason for using copper metal particles is due to its excellent conductivity properties. A copper wire has an electric conductivity of $5.95 \times 10^7 \frac{1}{\Omega m}$. The conductivity of an oxidized copper particle varies with its level of oxidization. This is the principle used to drive the sensing of corrosion of a certain metallic structure. Copper (I) oxide is used as the active element in the corrosion sensor sensing material. This is possible because its electric resistivity changes with the amount of oxide surrounding the particle, which varies with time of exposure to a corrosive environment. The conductivity variance is what indicates the oxidation level of a metallic structures exposed to the elements. Copper (I) oxide is brown whereas native copper has orange like color as seen in figure 6. The electrochemical reaction of copper to copper (I) oxide is as follow:

$$4Cu + O_2 \rightarrow 2Cu_2O \qquad (1)$$

With an oxidation reaction of copper atoms consisting of,

$$Cu \rightarrow Cu^{+2} + 2e^{-} \qquad (2)$$

And a third and complimentary reaction of the oxygen atoms admitting 2 electrons thus changing into oxygen ions,

$$O_2 + 4e^{-} \rightarrow 2o^{-2} \qquad (3)$$

The distinct copper (I) oxide resulting from the above electrochemical reaction is shown below in figure 6. A more oxidized copper (oxidized at the second level) is called copper (II) oxide, cupric oxide, is darker and more oxidized, hence the darker color. Cupric oxide has one copper molecule per oxygen thus more oxide in total per mole of copper (II) oxide than what copper (I) oxide has. In order to reverse the oxidization process that the copper (I) oxide underwent, acetic acid is reacted with the copper (I) oxide to produce copper particles free of oxide.

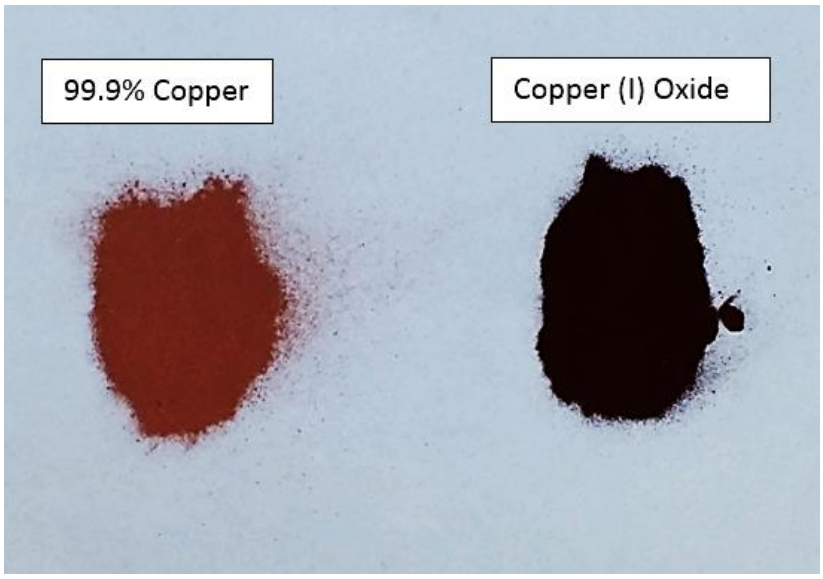

Figure 5: Native copper (left) versus copper (I) oxide (right).

The following chemical equation shows copper (I) oxide (Cu_2O) reacting in acetic acid (CH_3COOH) to form cupric acetate, water molecules, and hydrogen.

$$Cu_2O + 4CH_3COOH \rightarrow Cu(CH_3COOH)_2 + H_2O + H_2 \quad (4)$$

The resulting effect is that copper is oxide free and is not prompted to re-oxidization from the environment it is in (as observed by Chavez and Hess) [6] even though embedded in an inert polymer. [6] The polymer in question has a critical role in manufacturing and characterizing the sensing device and will be discussed shortly. It has been observed that ionized copper was present in the solution bath used to remove the oxide from the copper (I) oxide particles, hence the blue colored acetic acid solution, see figure 35. Copper particles embedded in the sensing material are used to conduct an electric signal. The electric signal follows a path created by a string of particles randomly aligned within electron transfer distance. It has been observed that only the 80% weight/ total weight of copper in polydimethylsiloxane (PDMS) have the ability to conduct electricity.[7] All other lower percent compositions are not able to conduct a measurable electric current. Due to the fact that higher percent compositions are difficult to fabricate, only the 80% weight / total weight of copper in PDMS is assumed to be the optimum sensing material composition that can conduct electricity. The embedded copper particle are assumed circular (though they are flat and ellipsoidal), with an average particle size ranging from 8-11μm.

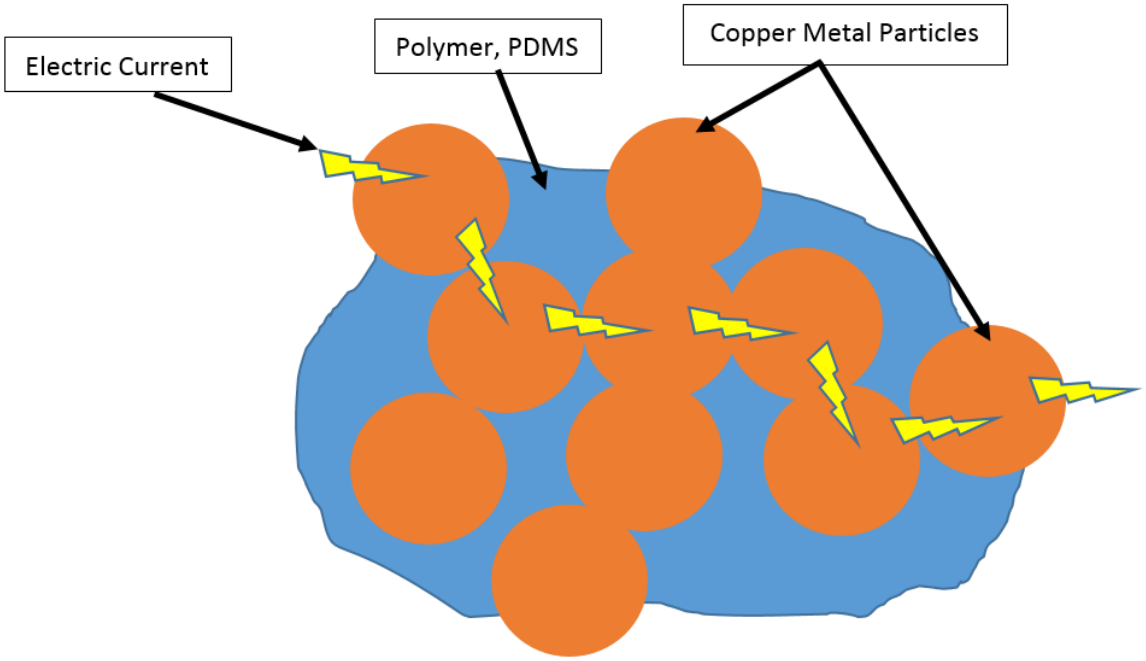

Figure 6: Current path through PDMS matrix via deoxidized copper particles.

The electric current, represented in yellow lightning bolt, follows a randomly made path that goes from one end of the composite to the other, thus carrying the current from one end to the other. It is that current which will, overtime, be reduced because of the oxide built up around the copper particles. The polymer separating the copper particles is represented in blue and the copper particles in orange. It is verifiable that the higher the weight percent composition the more likely the sensing material is to conduct electricity. This principle is essential for controlling the corrosion sensing and is discussed in the following section.

2. Polymer for Sensing Control

Polydimethylsiloxane (PDMS) is used for controlling the oxidation rate of the copper particles. This is done by varying the weight or mass percent of copper particles to PDMS composite. PDMS is used for protecting the copper particles from premature oxidization. Its polymeric chains

envelop the copper particles thus retarding any reactive molecule present in the environment from having access and reacting with the copper particles. Just as a plastic wrapping protects its content from water vapor in order to preserve that content, the PDMS is protecting the copper particles from the oxide that would otherwise oxidize it within minutes.

PDMS chemical formula consists of n (between 90 and 140 times) repeating dimethylsiloxy $(CH_3)_2SiO$ with trimethylsiloxy $(CH_3)_3SiO$ ending both ends of the string of dimethylsiloxy [8].

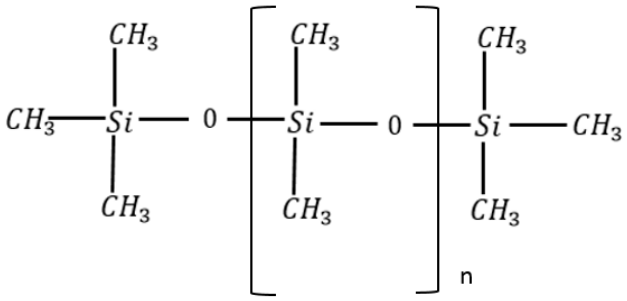

Figure 7: Polydimethylsiloxane string of n-dimethylsiloxy ended at both ends with trimethylsiloxy molecules. *(8)*

PDMS does not occur naturally and is made with a silicon content ranging between 37.3% and 38.5%. It has a specific density ranging from 0.964 to 0.977 [8] (compared to the density of water of 999.97 kg/m^3 at room temperature (~ 20^o C)). CH_3 called Methyl cellulose is the most common element in the PDMS chemical structure. It is also not natural and is artificially made. It is the element that gives the gelatinous properties to PDMS to where when heated it solidifies. This property of PDMS was used to accelerate the fabrication process of the copper composite corrosion sensing device and will be further discussed in the following sections. The Methyl cellulose also gives the PDMS a hydrophobicity property, which essentially prohibits water molecules from penetrating its structure once cured and solidified. The water solubility of PDMS prior to its

solidification is not known. PDMS is soluble in toluene and some other organic solvents. This is useful for developing our corrosion sensing device especially because toluene is the transport agent that carries and creates pathways through the PDMS matrix for the etchant, acetic acid, to have access and thus remove the undesired oxide from the native copper particles embedded in the PDMS matrix. This development step is crucial for the functionality of the corrosion sensing device. Acetic acid, used as the etchant, cannot on its own carry out the de-oxidization process because the impermeability of the PDMS structure does not allow it to do so. Choosing PDMS as a control, housing, and inert second element for fabricating the corrosion sensing device has been justified in the prior paragraph. PDMS also happen to be the most commonly used elastomer for fabricating Nano/micro channels in MEMS (Micro Electro-Mechanical Systems). It is also inexpensive compared to other potential candidates. Its availability perfectly aligns with one important goal of this corrosion sensing device development, which is to make the device sufficiently inexpensive that it is available to any interested parties.

Chapter 3. Sensing Material Development

Once the critical element for sensing corrosion have been picked and understood, the fabrication of the actual shape and form sensing material was undertaken. The sensing material is still not yet being prepared for installation on its actual mount, which has not been yet developed. The sensing material is currently fabricated for characterization only. A shape that is easy to obtain and is as accurate as possible is a disc. A 1 mm or 0.04 inches thick mold consisting of nine pockets (Figure 9) is used along with two metal plates as molds for fabricating the sensing material. This allows the fabrication of multiple different percent composition of copper to PDMS. The characterization goal was set to experiment on copper wt. % over total wt. % ranging from 20% to 80% at increments of 10%. With a mold that had nine pockets, variation during fabrication was minimized to where the PDMS base element, the temperature, and curing time were virtually identical. That indeed made significant differences in the data itself, as explained and demonstrated in the First Experimental Data section. The fabrication process proposed by Pan et al. (2007) in his doctoral dissertation was adopted here as mean of replicating the data previously acquired. This was intended for validating the work that Pan had already done for his doctoral dissertation.

1. Sensing material fabrication

The first fabrication step undertaken was the PDMS (10:1 ratio PDMS oil to its curing Agent). Once those have been thoroughly mixed, for about 5 minutes, the mixture is degassed at 25 mili-torrs, which is one thirtieth the atmospheric pressure, for about 10 minutes. This step is taken to aid with homogeneous curing during the pre-curing following step. After being degassed for 10 minutes, the PDMS mixture is baked at 80^{o}C for 4 minutes. This process was implemented to increase the settling time of the copper particles in the PDMS mixture, which then became a gooey like solution. A copper particle weights is greater than the buoyancy force exerted on it, thus

causing the particle to sink at the bottom of the mixture. This settling is undesired and would cause the sensing material to malfunction. Once cured, the PDMS mixture was again degassed until there was visibly no more bubble in the mixture.

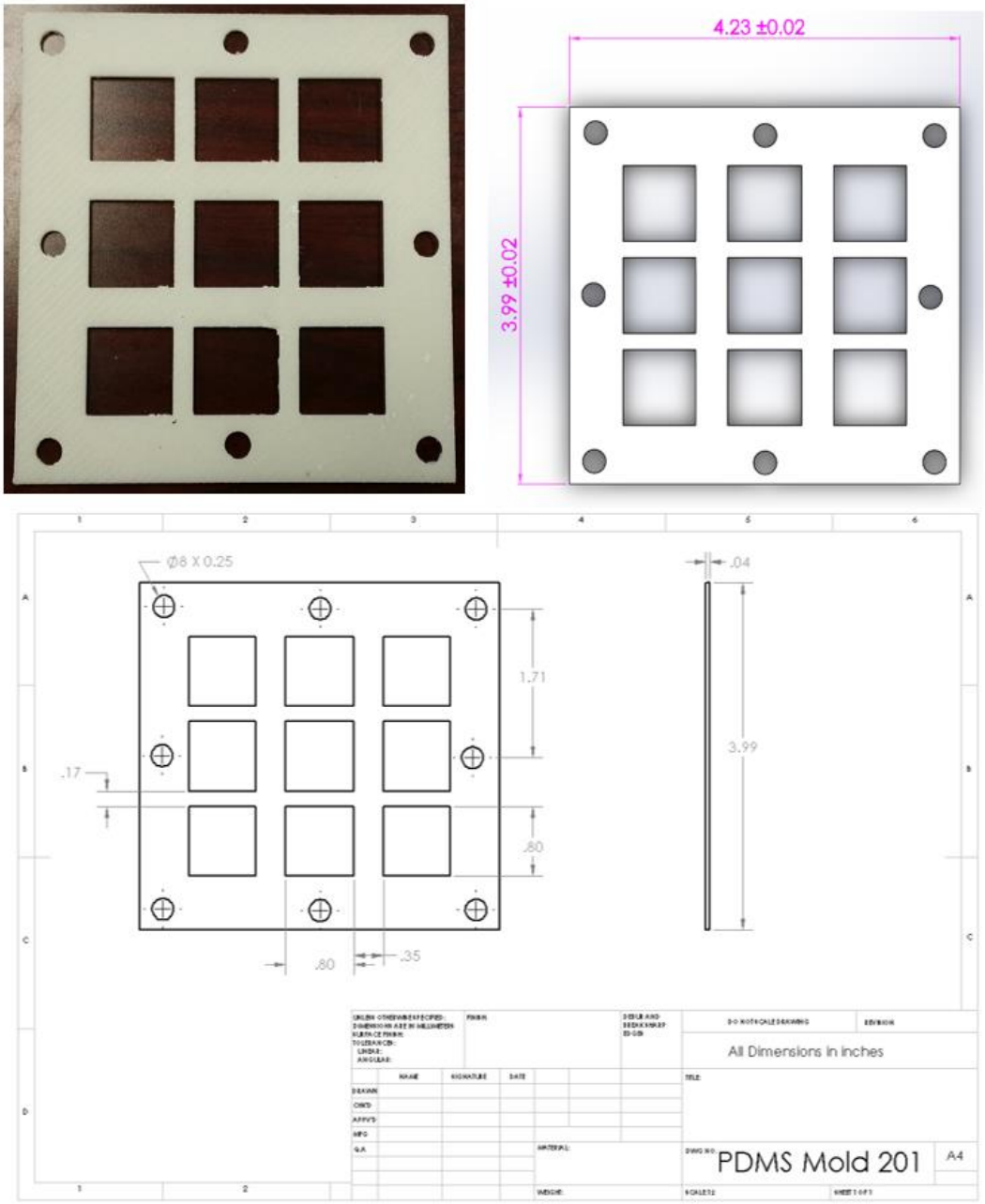

Figure 8: Copper-PDMS composite ABS-P430TM mold

One predominating fabrication malfunction would be the non-uniform swelling of the copper-PDMS composites. This will jeopardize the swelling data acquisition method, thus compromising the data acquired. The second fabrication process consists of mixing the copper particles to the pre-cured PDMS mixture. A Mettler Toledo one thousandth gram accuracy jewelry digital scale was used for accurately measuring the weight of, first the copper particles to their appropriate weight for the appropriate percent concentration, then the copper particles and PDMS mixture once the PDMS mixture was poured into the container. The level of accuracy of the composite is not verifiable with the current setup available at Dr. Huang's Laboratory; therefore, the percent composition was assumed to be accurate. A preparation time of about fifteen minutes was allocated for weighting and mixing the copper particles to the PDMS mixture. This was done so that all seven different percent compositions could all be done at once and taken to the next step at about the same time. Once weighted, the copper particle and PDMS mixture is thoroughly mixed, poured into the mold, closed with the aluminum plates, and solidly packed in by tightening eight bolts on the aluminum plates. The mold is then sent into the microclimate climate control chamber to cure for approximately one hour at 60^{o}C. The third and last step of the fabrication process is to punch out the sensing materials final shapes with a 1/4 inch (6.35mm) diameter whole puncher. Note that all composite samples where obtained from the same batch of PDMS mixture to ensure that benign fabrication variables would not affect the accuracy of the data obtained. For example, the curing agent added in the PDMS oil would be relatively different for every batch made. The amount of curing agent dictates to some extents the end physical property of the cured PDMS. The assumed error can be avoided by using a more automated fabrication process and with more precise measuring instruments.

Figure 9: Mettler Toledo thousandth gram digital scale and a one-hole hole-puncher.

2. Oxide Removal Process and Parameterization

Now that the copper particles have been fabricated and have been allocated sufficiently enough time to fully cure, the oxide removal process was undertaken. Note that old and extensively oxidized copper (I) oxide particles were used and that was for optimum parameterization and to ensure that all data obtained reflect scenarios where the copper particle are fully oxidized. This is in fact the maximum oxide layer a copper particle can possibly have at once. The goal is to remove as much oxide as possible by a swelling-etching sequential or simultaneous process. Two methods for conducting that process were implemented. The first method used the basis that the swelling should lead into the process prior to adding the etchant. This lead to experimenting with the solvent

alone in order to fully understand the expansion parameters of the composite, which will then allow us to appropriately design a process for etching the oxide according to the first method proposed. The oxide removal was proven by previous work to where the oxide removal progression was monitored and recorded for copper to PDMS composite coupons. The coupon, used for proving the oxide is actually being removed, was submerged into an acetic acid bath and monitored by collecting data, scanned in with a scanner, every 30 minutes for a total of two hours, shown in figure 11. [7] It was proven that the etchant does in fact remove the oxide over time. Represented in red array, the de-oxidized copper progressively moved in the same direction as the diffusion, as shown by the yellow arrow in figure 11, at a slow rate. Though it was clear that the oxide is in fact being removed, the rate at which it did so was unsatisfactory and needed to be accelerated. That is the reason why a facilitator, swelling agent or solvent, was added to the oxide removal process to accelerate the process.

a. Swelling Agent (solvent) and Cohesive Energies

The next step for the experimentation was to choose an appropriate swelling agent (solvent). For this, the cohesive energies of five solvents were studied. The cohesive energy of a material is the energy required to dissociate its molecules, thus breaking the bonds that connect molecules, within that material, from one another. The cohesive energy is derived from the Energy of Vaporization equation.

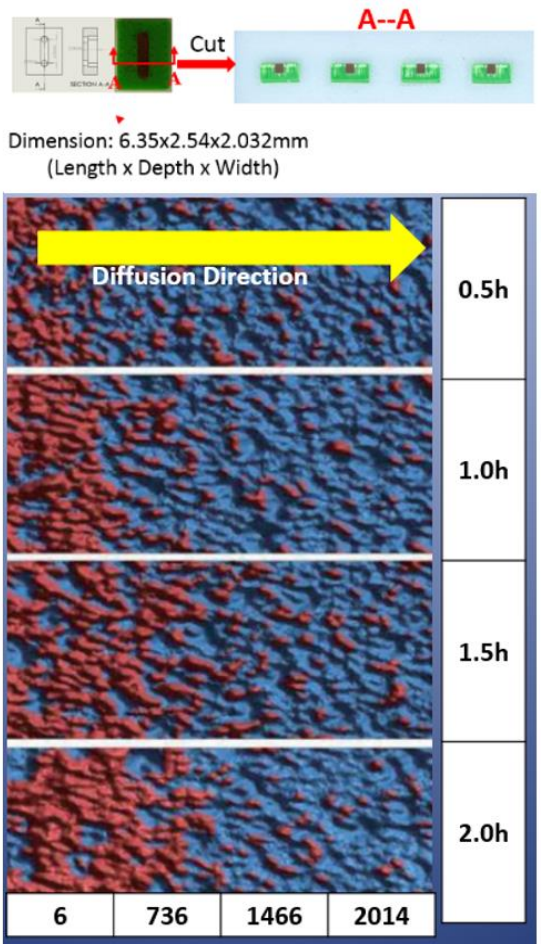

Figure 10: Oxide removal progression of copper-PDMS composite samples. [7]

The Energy of Vaporization is the summation of the three solvent numbers, also called Solubility Parameters or Hildebrand Parameters.

$$E = E_d + E_p + E_h \quad (5)$$

Where E is the energy of vaporization; E_d the dispersion (London) forces; E_p the permanent dipole-permanent dipole forces; and E_h the hydrogen bonding forces. These parameters are assumed to have all the necessary forces acting on and within the material to alter any physical properties the material may have. The energy of vaporization is divided through by V, the molar volume.

$$\frac{E}{V} = \frac{E_d}{V} + \frac{E_p}{V} + \frac{E_h}{V} \quad (6)$$

From there the cohesive energy equation is derived as follow:

$$\partial^2 = {\partial_d}^2 + {\partial_p}^2 + {\partial_h}^2 \quad (7)$$

Where $\partial = \sqrt{\frac{E}{V}}$ the cohesive energy is what dictates the energy needed for breaking the bonds of a material in order to dissolve it in another material. Note that the cohesive energy also dictates the compatibility, or dissolvability, of two materials. This is the concept used for choosing the appropriate solvent for aiding the oxide removal process for the corrosion sensor development. $\partial_d = \sqrt{\frac{E_d}{V}}$ is the dispersion energy component, $\partial_p = \sqrt{\frac{E_p}{V}}$ the polar energy component, and $\partial_h = \sqrt{\frac{E_h}{V}}$ the hydrogen-bonding energy component. All units are in Mpa ^{½}.

Table 2: Cohesive parameters for toluene, acetone, methanol, isopropyl alcohol, and 1-methoxy-2-proopanol acetone (Su-8 Developer).

Solvent	**∂(Mpa $^{1/2}$)**	**∂_d(MPa$^{1/2}$)**	**∂_p(Mpa $^{1/2}$)**	**∂_h(MPa$^{1/2}$)**
Toluene	**18.2**	**18.0**	**1.4**	**2.0**
Acetone	**20.0**	**15.5**	**10.4**	**7.0**
Methanol	**29.6**	**15.1**	**12.3**	**22.3**
IPA (Isopropyl alcohol)	**24.5**	**16.0**	**6.8**	**17.4**
1-Methoxy-2-Propanol Acetate (SU-8 Developer)	**18.8**	*****	*****	*****

The cohesive energy of PDMS liquid (oil) is ∂=14.9MPa$^{1/2}$. Based on the compatibility or dissolvability theory, toluene is indeed a better match for PDMS, even though PDMS is in its liquid oil form. This choice is justified for the fact that the maximum expansion is sought and toluene is in fact the solvent which will growth the PDMS samples to their maximum size. The graph below obtained from Pan et al. (2007). (2007) doctoral dissertation does indeed empirically prove that toluene will grow the PDMS sample the most, thus providing the best material transport through the PDMS's matrix. [7] Toluene registered and maximum expansion of over 30% whereas the next highest expansion registered by acetone is less than 10%, as seen in figure 13. Toluene would undeniably grow the PDMS samples to their maxima. [7]

a. Swelling Parameters

PDMS is an inert polymer and insoluble in water when cured with its curing agent at a certain temperature. Though insoluble in water, PDMS is soluble in toluene, which will actually expand the PDMS matrix creating essential paths needed for channeling the etchant to the copper (I) oxide, embedded in the PDMS matrix, for de-oxidization. In order to empirically decide when to add the etchant, the swelling parameters of the copper to PDMS composites were acquired. This process consisted of submerging the copper to PDMS composites into the toluene for 12000 seconds, record data every 500 milliseconds or at a frequency of 2 Hz, plot and curve fit the data with a two terms exponential model. The first term gave the maximum expansion and the main time constant for the expansion curve, which are both essential for implementing the etching process.

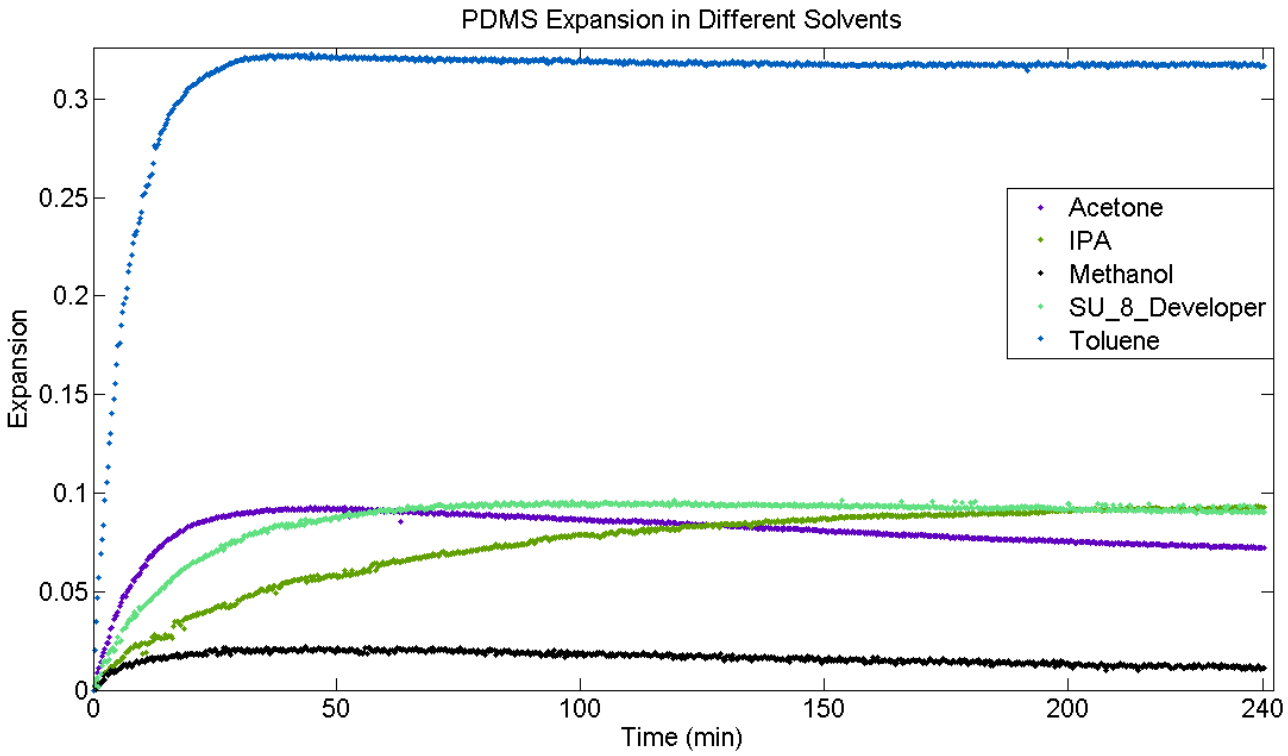

Figure 11: Expansion curves obtained for pure PDMS (no particles added) for five different solvents. [7]

In addition to knowing precisely when to add the etchant, the common batch fabrication method has been confirmed through the data obtained, as seen in the data and results section chapter 5. The second etching process methodology essentially explored the opposite and more direct method for etching the oxide. That method consisted of adding the etchant along with the toluene without any waiting time. The best and more direct technique for doing that is to premix the acetic acid, etchant, to the toluene prior to submerging the copper to PDMS composite samples in the solution. This method has proven to expose some interesting material and physical properties of the copper to PDMS composite and the phenomena of oxide removal from an inert housing with changing stiffness.

b. Oxide Removal Parameters

Once all data are obtained and compiled into tables and graphs, understanding the oxide removal parameters of all copper (I) oxide to PDMS composite percentages was the ultimate goal for this research work. The successful completion of this research was essential for developing the corrosion sensing device. The sensing capability, but not only just that, depends on how much oxide remains on the copper particle once the sensing material is fabricated. This is essentially where the sensing parameterization began and dictated how effective this novel corrosion sensing technique is for a given scenario. The main oxide removal parameter needed is the faster and more effective oxide removal process. Due to a lack of time, only two methods were attempted, see part a. above. It is clear that more oxide removal processes can be undertaken with different sample sizes and other fabrication parameters. Note that the corrosion sensor is still under development and is nowhere near completion and or implementation. Although insignificant with regards to the work that remains to be done, the two oxide removal processes proved to be sufficient for the time being. A logical step following the above sections is to find a relation between impedance across the copper (I) oxide to PDMS composite samples and oxide removal processes. This is where the most optimum process is finally picked for implementing the device. This entire step will be left unexplored for it is currently beyond the scopes of this research objective and will require much more time and effort to be carried out properly.

Chapter 4. Data Acquisition Systems

1. System Set Up

LabVIEW™ and Matlab® were used to collect the experiments data. LabVIEW™ was programmed to use a Microsoft LifeCam 6 Channels 00001 camera 720p 30 frames per seconds to acquire the images, then processed internally using LabVIEW™ Vision Assistant™ package. The entire process is done in a chronological order as depicted in the following diagram.

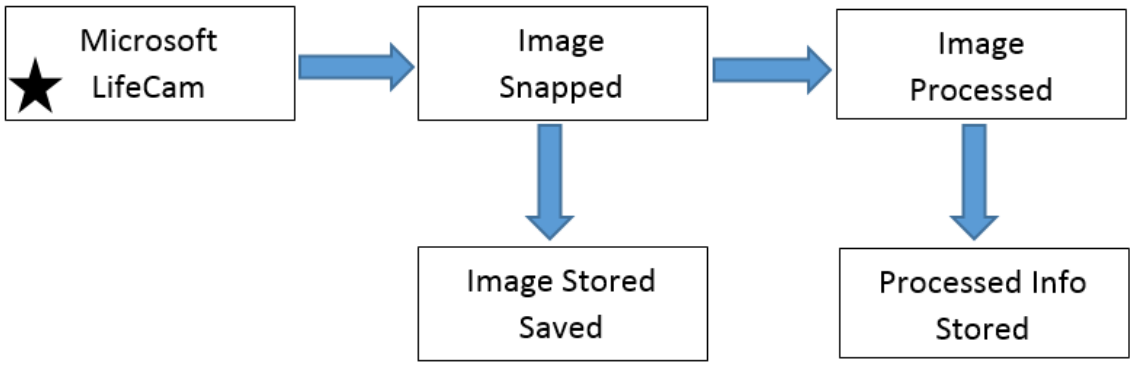

Figure 12: Image Acquisition Process Diagram

The star in the first box represents the default starting point of the process. That is the first step of the LabVIEW™ program where lines of code initiate the camera by finding its IP address, turning it on, and shutting it down when the process has completed. The diagram shown above is a rugged flow process highlighting the major processing steps of the set up.

a. Self-centering apparatus

A self-centering apparatus was used to ensure repeatable data acquisition. The self-centering apparatus align both the camera and the receptacle, a flat bottom beaker, on their axis of rotation.

This allows the receptacle to be removed, cleaned, and replaced without off centering the camera thus minimizing calibration efforts.

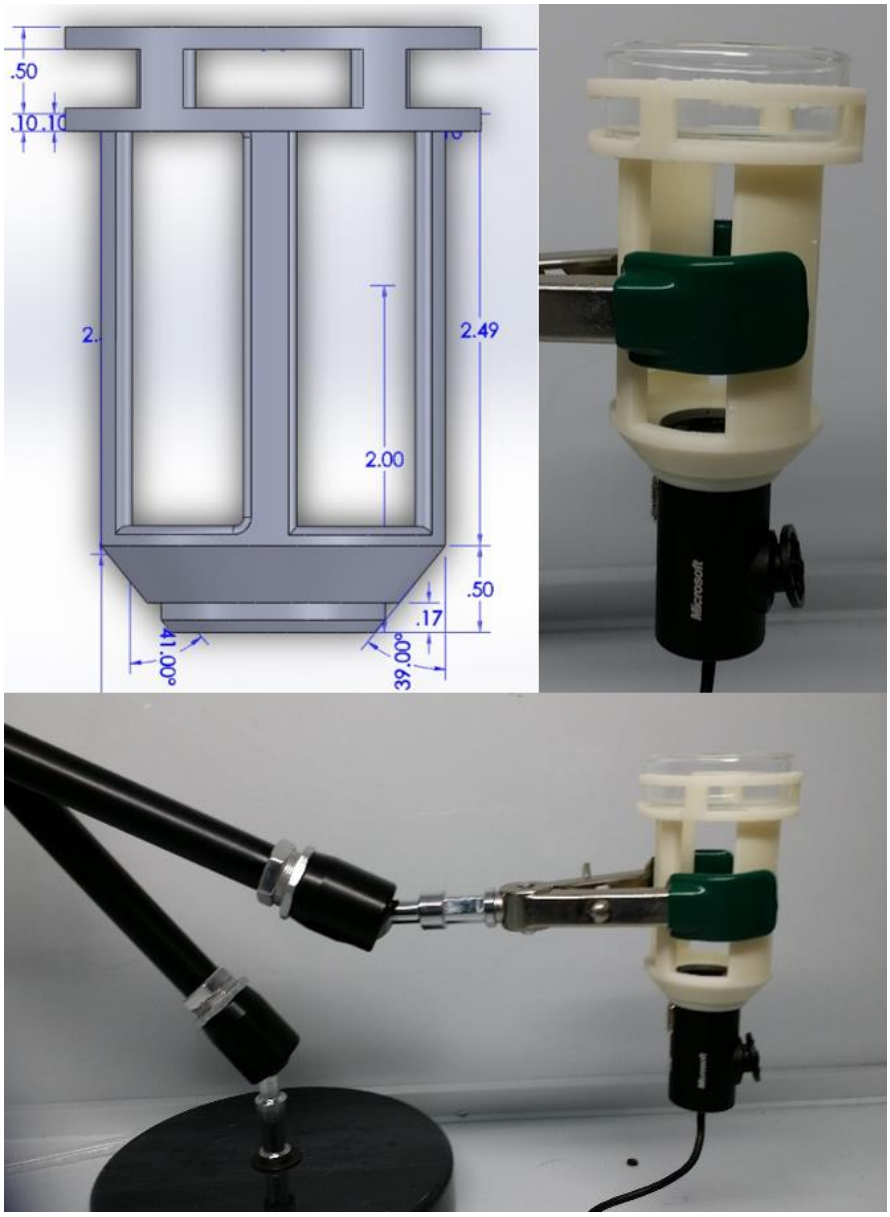

Figure 13: Self-Centering Apparatus (all dimensions in inches).

The Self-centering apparatus is 3D printed with ABS-P430 XL Model (Ivory) building material. It is designed to press fit the camera and the beaker. That allows for the beaker to be removed and replaced effortlessly when it needs to be cleaned.

b. Camera

The camera used for the image acquisition is a Microsoft LifeCam camera. It is an inexpensive camera that has the capability to acquire sufficiently well-defined images, at rate of 30 frames per seconds that could then be analyzed to obtain accurate data. The camera is mounted through the bottom of the self-centering apparatus at a preset distance, set by the apparatus. The Microsoft LifeCam has two operating instances which are take pictures and record movies. It is used as a camera-recorder programmed in the LabVIEW code used for the experiment. Its picture acquisition capability was previously used to program LabVIEW but due to its instability, it was discarded and replaced with its recording capability. Once the camera is started, it remains on the entire image acquisition period. The LabVIEW program uses a few lines of code to fetch for a frame, from the frames being recorded, without interrupting the camera's recording process.

2. LabVIEW

LabVIEW is a virtual process control instrument used to control the data acquisition elements of the experiment. LabVIEW uses a PLS (programmable logic control) logic language that has a C++ based block language to send and receive instructions (signals) or information to and from the elements it controls. LabVIEW main software has two interfaces that its users can utilize to one – program the logic for their system called the Block Diagram, and two – design an operator interface called the Front Panel, which is what holds all indicators and controls of the system. LabVIEW also has a Vision Assistant software that allows programmers to develop a code that uses images either downloaded from a folder or directly acquired from USB devices (cameras for example) or other computer devices such as spectrophotometer and thermal infrared devices. The vision assistant software lets programmers design an image analysis flow process then convert it into a .vi extension file, which would run on the main LabVIEW software. Note that a similar flow

process can be built directly on the main LabVIEW software. LabVIEW has other suites that deal with robotics, motor control, and an industry PLC suite. LabVIEW can also be used to run simulations.

a. Binary Image Acquisition

The swelling of the Copper-PDMS samples is measured using a camera controlled by LabVIEW. A Microsoft Live Cam is used with LabVIEW to record the swelling of the samples. Although inexpensive, the camera used basic capability was enhanced with advanced LabVIEW programming.

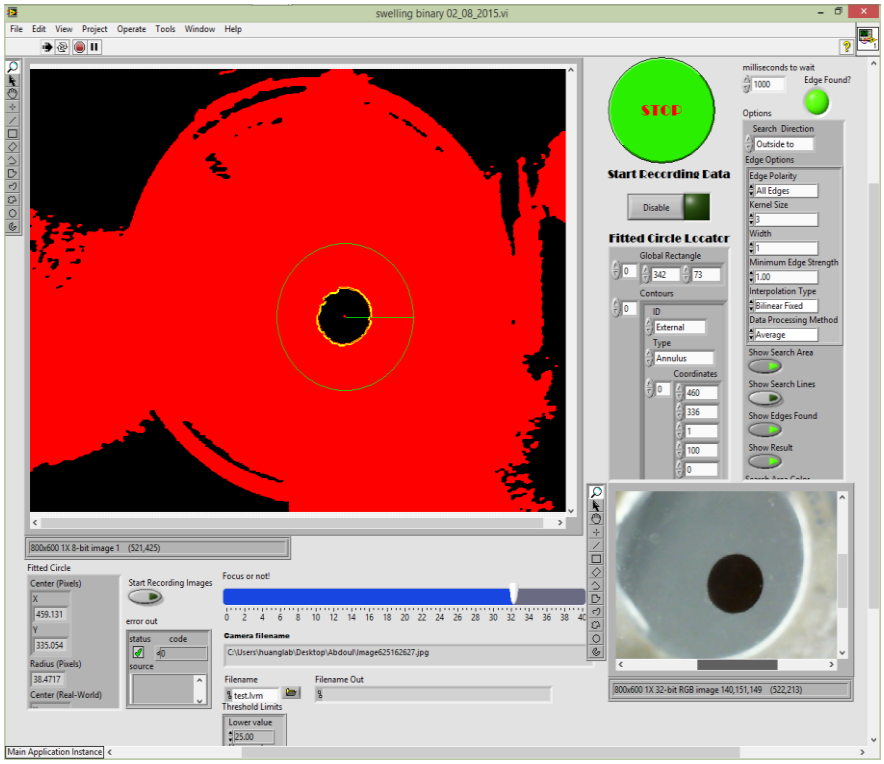

Figure 14: Binary Swelling Acquisition Front Panel.

The size of the sample is measured using the pixel size of the image. Several image processing steps were taken to condition the image prior to measuring the size of the sample. The acquired

image is changed into a grayscale, in a first instance, from the RGB (Red 64%, Blue 32%, and Green 2%) image spectrum. [9] An RGB image is what one would see on color photos. It uses a complex assemblage of multiple intermediate shades between the Red, Blue, and Green colors to represent images on a Cartesian coordinate system. An intermediate step was taken to transform the Cartesian coordinate system to Hue Saturation Lightness cylindrical coordinate system. [10] This is a common image processing practice which allows images to be processed easier than on a Cartesian coordinate system. On a Cartesian system every color intensity is represented in order to process every pixel, but the cylindrical system allows a color to be represented with the Hue Saturation Lightness elements. [10] A grayscale image is one that is wholly defined by two colors, black and white. Such images are also known as binary images because they are represented by only two distinct colors. Though represented by only two colors, grayscale images are formed of multiple shades of gray as seen in a black to white spectrum. Note that LabVIEW™ allows us to select a color plane on which the transformation happens. Essentially the other colors, blue and green, are removed from the image. Transforming the acquired image in a two tone image allows us to transform it further in to a 0-1 binary image representation. The shade intensity or light intensity of the pixel is measurable and thus controllable. Setting a light intensity threshold allows the lighter gray to be segregated from the darker gray thus setting a binary on or off/true or false like image representation. A true pixel is seen as red and false pixel seen as black.

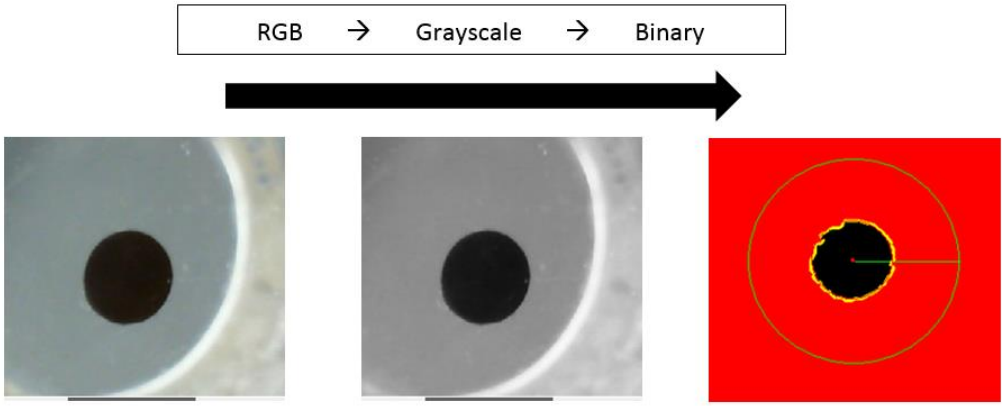

Figure 15: Image Transformation Process.

Controlling the threshold of the binary image has proven to be complex especially for the type of experiment proposed. As the samples swell, their size changed therefore changing the focus of the camera. That significantly distorted the initial threshold and calibration performed for the image acquisition. As a result the image transformed into binary was highly inaccurate and scattered, which led to modifying the image processing method.

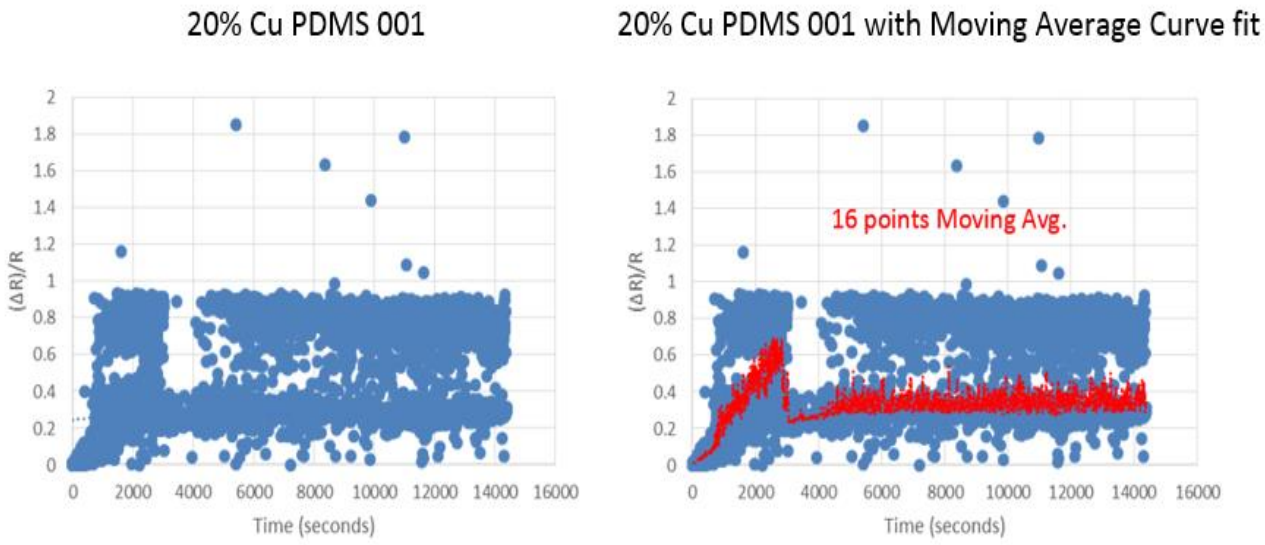

Figure 16: (Sample Data) First Test Data Recorded using the Binary Image Processing.

The above graphs show swelling results obtained with the binary image processing method. The swelling trend is present as represented by the curve fit, shown in red, but is not as clear as one would like it to be. The binary method is an advanced process which could be used to analyze images, but in this case, it is not a preferred process. A better understanding of threshold implementation for binary images could be beneficial for improving the binary image processing method.

b. Simple RGB and Grayscale Images Processing

In the simple RGB image processing RGB images are recorded then transformed into grayscale images.

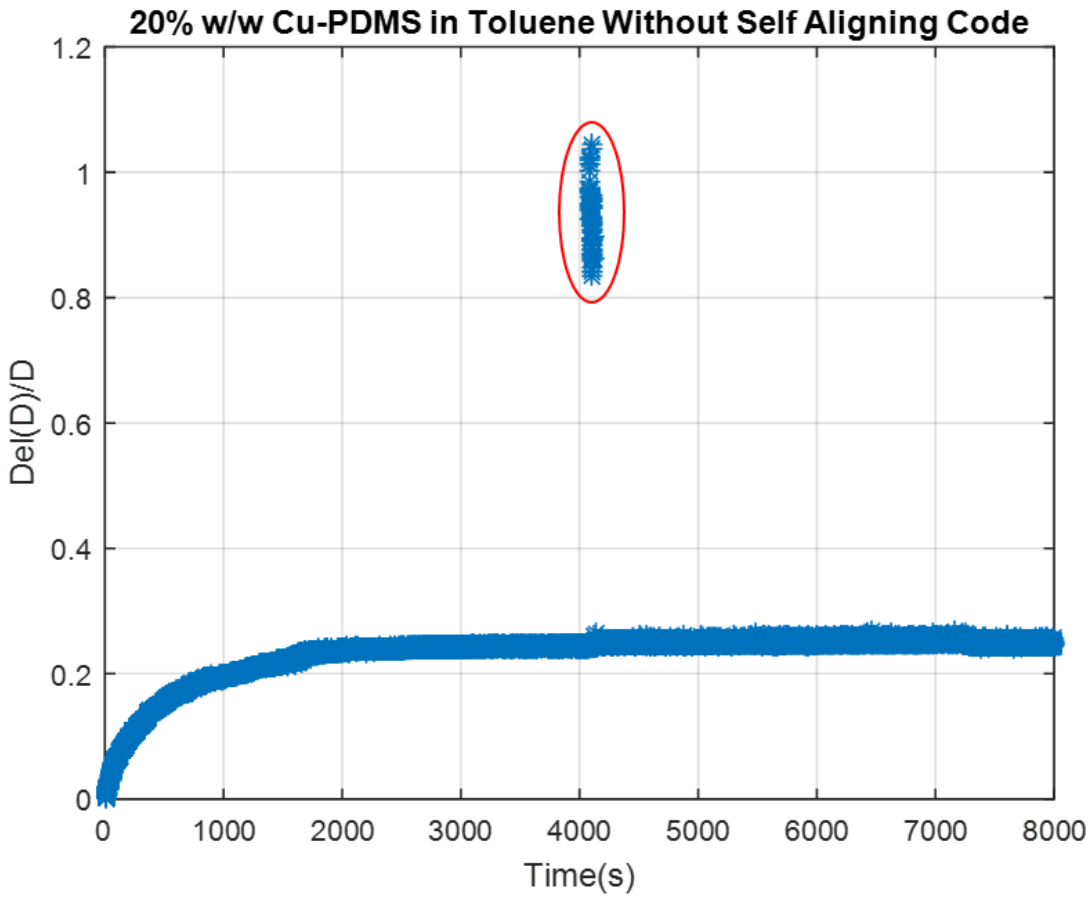

Figure 17: Second Test Data without Self Aligning Code.

The Cartesian coordinate system transformed into the HSL cylindrical coordinate system prior to the grayscale transformation. The binary transformation process is skipped as a whole. An annular ROI is added to the image then coded to sweep for circular contrasts. A manual focusing option is added to help with the stability and clarity of the images captured. The focus level does affect the initial pixel size of the sample and has to be taken in account every time the focus level is changed. The data circled above in the graph are miscellaneous data recorded during the swelling a 20% test sample where the sample would actually shift and alter the data acquisition process. It was caught on time and fixed manually. This issue repeated several times during the data acquisition process.

c. Self-Aligning Code

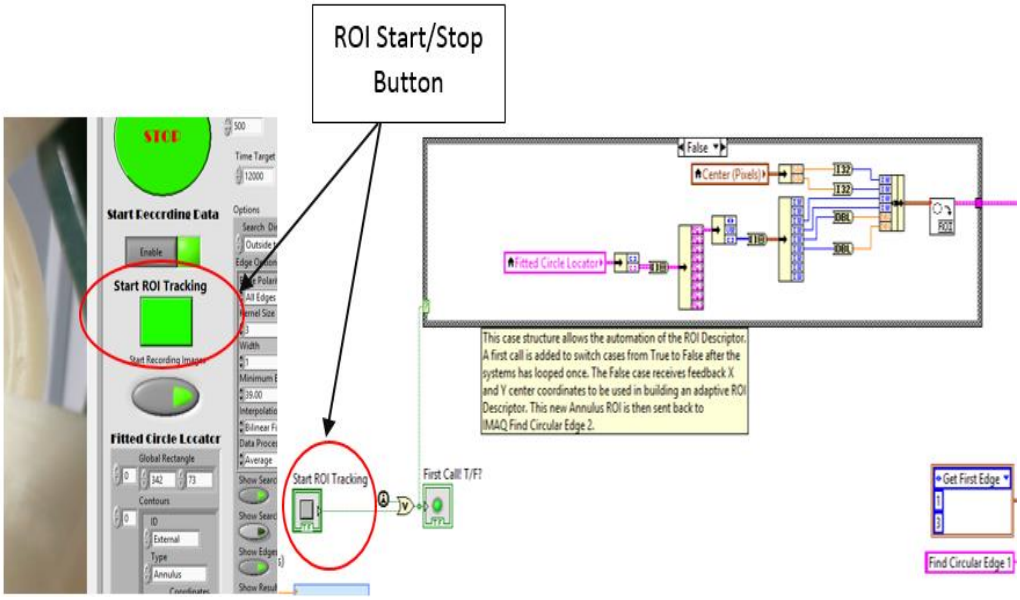

Figure 18: Self-Aligning Code portion the Block Diagram and Front Panel Start/Stop Button.

To contour the data acquisition issue, a self-aligning code was added to the LabVIEW ™ program. The self-aligning code repositions the ROI centering it to the sample using the coordinates of the fitted circle as a feedback. This method requires the sample to be properly positioned initially before the code can work as envisioned. A self-aligning start/stop button, on the front panel,

facilitates the initialization of the code. This code significantly improved the data acquisition process allowing the data to be much more accurate (95% repeatable).

d. Matlab® Codes

Once the data has been collected, Matlab® was used to analyze it and curve fit for obtaining the parameters sought. These parameters are especially important for development phase of the corrosion sensing device. Matlab® curve fit suite was used to facilitate the data analysis. A much more complex method of analysis could have been used involving the programming of nonlinear regression or a piecewise curve fitting methods. Matlab® suite contained a two exponential terms that perfectly fitted the expansion curve obtained from the experiments. That allowed us to remain consistent with the previously obtained data from Pan et al. (2007). (2007). This Matlab® code proved to be efficient. It loaded data1 .mat file, which contained all the data gathered for the composite in question. It then used the two user defined data sets in a normalizing loop. Once the data was normalized, it was curve fitted using the Matlab® - fit – function for a two term exponential curve, represented by "exp2." Though the Matlab® implemented did properly analyze the data it was handed to, a minor misrepresentation was noticed. The first Matlab® code used to analysis the data is as seen in Appendix 4. It is implemented that the data be normalized using the first data it recorded. This was incorrectly implemented. The samples, once immerged in the bath, had a few seconds to a few minutes to swell and increase before the Start Recording button was pushed in. Enough time had passed that normalizing it with the first data recorded would be inaccurate.

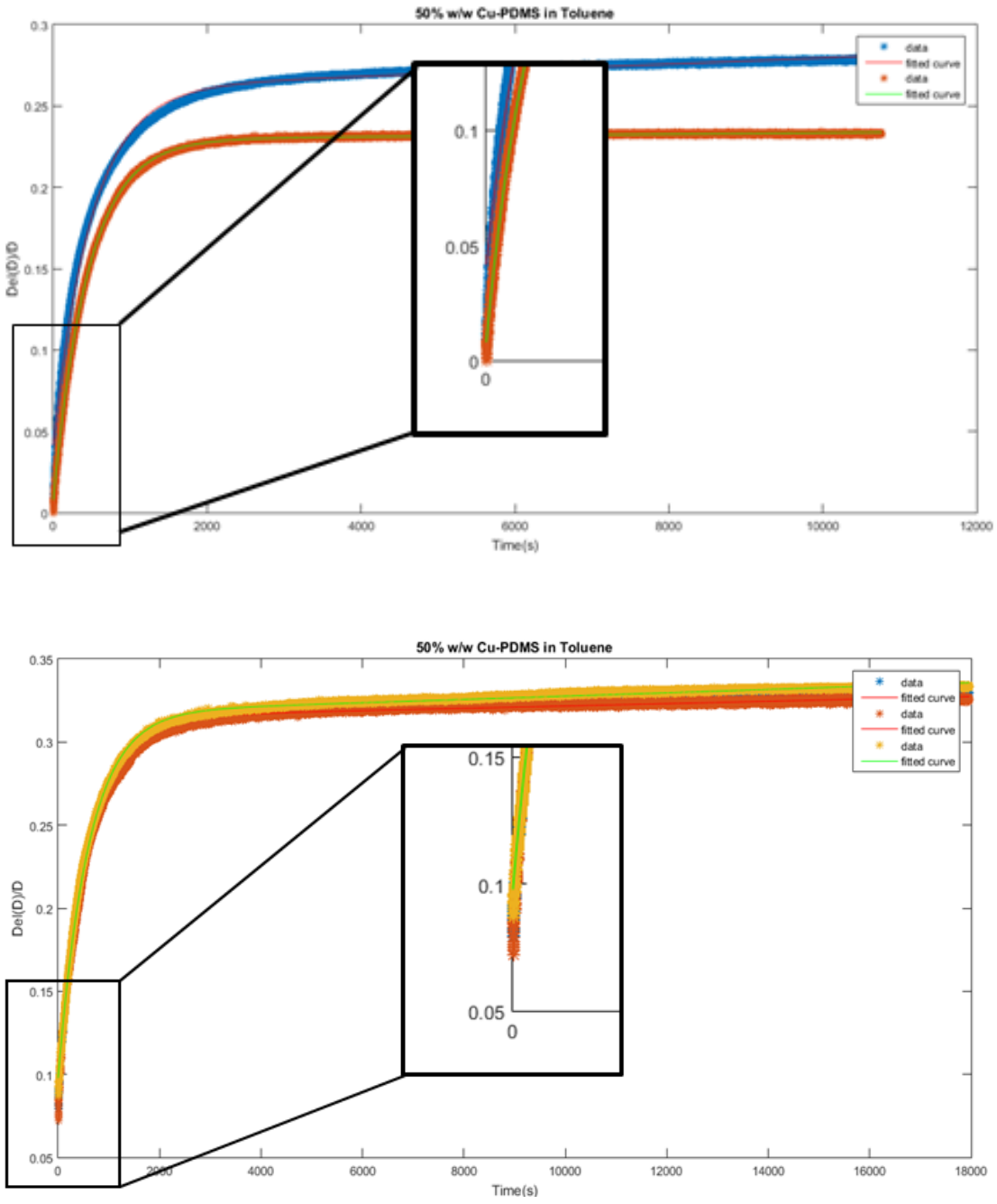

Figure 19: Comparing the variance in choosing a proper initial data point.

Figure 20 above show how the data could be misrepresented if the proper initial size, of the composite sample, is not used. The plot on the left shows the data starting at a zero, the origin, whereas it is known that the sample had time to grow before any data is recorded. The actual initial

size should be obtained outside of the bath, for the used focus set up. The focus on the image will actually change the initial size of the sample and thus need to be taken in account when finding the initial size of the composite. Once measured the initial sample size was added to the Matlab® code along with some minor changes to allow a clear and concise data analysis.

As seen in appendix 5, "R" represents the initial size of the sample and is used to normalize the data. Note that this is the pixel size of the as it is not measured but virtually represented via pixels. That is the reason why the focus on the image affects the initial size of the sample. Though varying with the focus level, the initial size will not change during the data acquisition, unless the focus level is manually changed to a different value.

Once all the desired data were gathered, a sum compiler was implemented to plot all the data together. Only the averages of each data set were plotted. The averages were obtained from the normalized values of each data set. The compiler was programmed as seen in appendix 6.

e. First experimental data

In order to demonstrate that the curing process is essential for fabricating adequate copper-PDMS composite samples, an experiment was run using composite samples that did not undergo the curing process and degassing process. This is relevant because it align with our goal for fabricating as cheaply as possible the corrosion sensing device. Not having to go through the degassing and the curing process would indeed minimize fabrication time and allow us to produce more samples per given time. Note that only the toluene swelling experiment was run and that no etching process was carried out for this step.

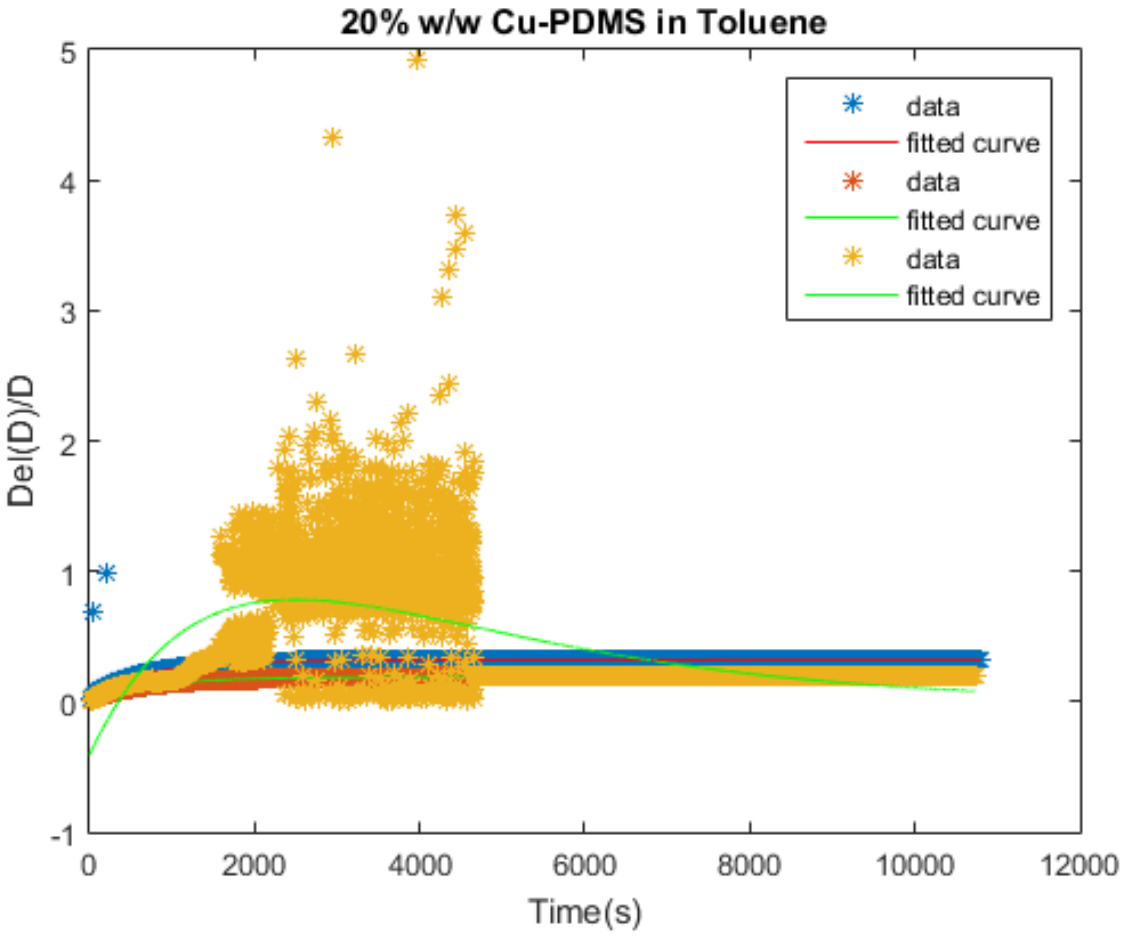

Figure 20:20% wt. /total wt. copper composite that did not undergo the pre-curing and degassing process.

Three 20% wt. /total wt. copper composite samples were grown in toluene for about 11,000 seconds or about 3 hours. The yellow data has the most discrepancy of all three sets of recorded data. A possible cause was that during the data acquisition for the yellow data set, the sample folded over thus changing the focus settings on the vision code. That made the edge finder to not recognize the edge contrast which caused the edge finder to randomly find any edge within its ROI (region of interest). Once the sample reached a certain growth size, it flattened out to its original

form. The edge finder then picked the right edge contrast and zeroed on to the appropriate edge to fit.

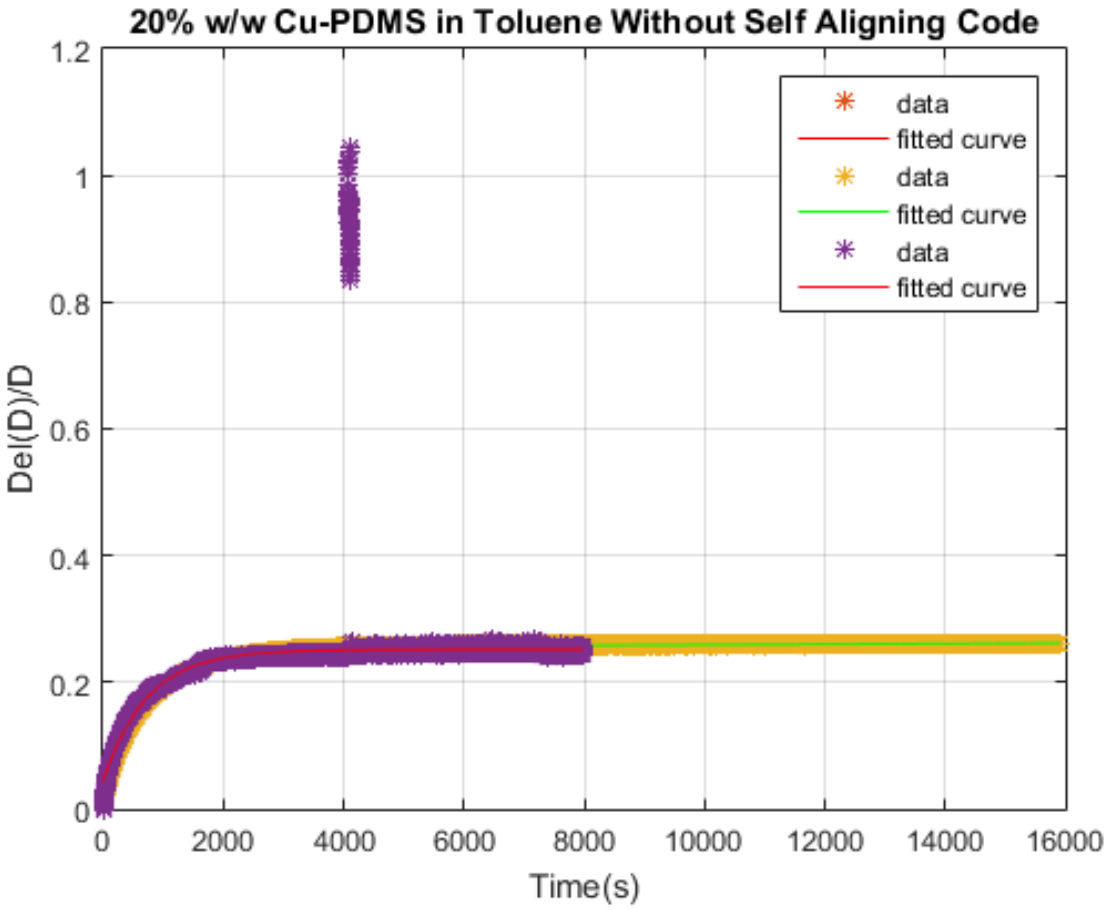

Figure 21: 20% wt. /total wt. copper composite that underwent the pre-curing and degassing process.

Comparing figure 41 to figure 40, it is clear that the fabrication process does in fact affect the quality of the data acquired. All data acquired precisely superposes on each other proving the conciseness in the composite samples. The degassing and pre-curing process does in fact improve the quality of the by removing excess gas locked into the PDMS and help with distributing the samples more uniformly into the PDMS matrix.

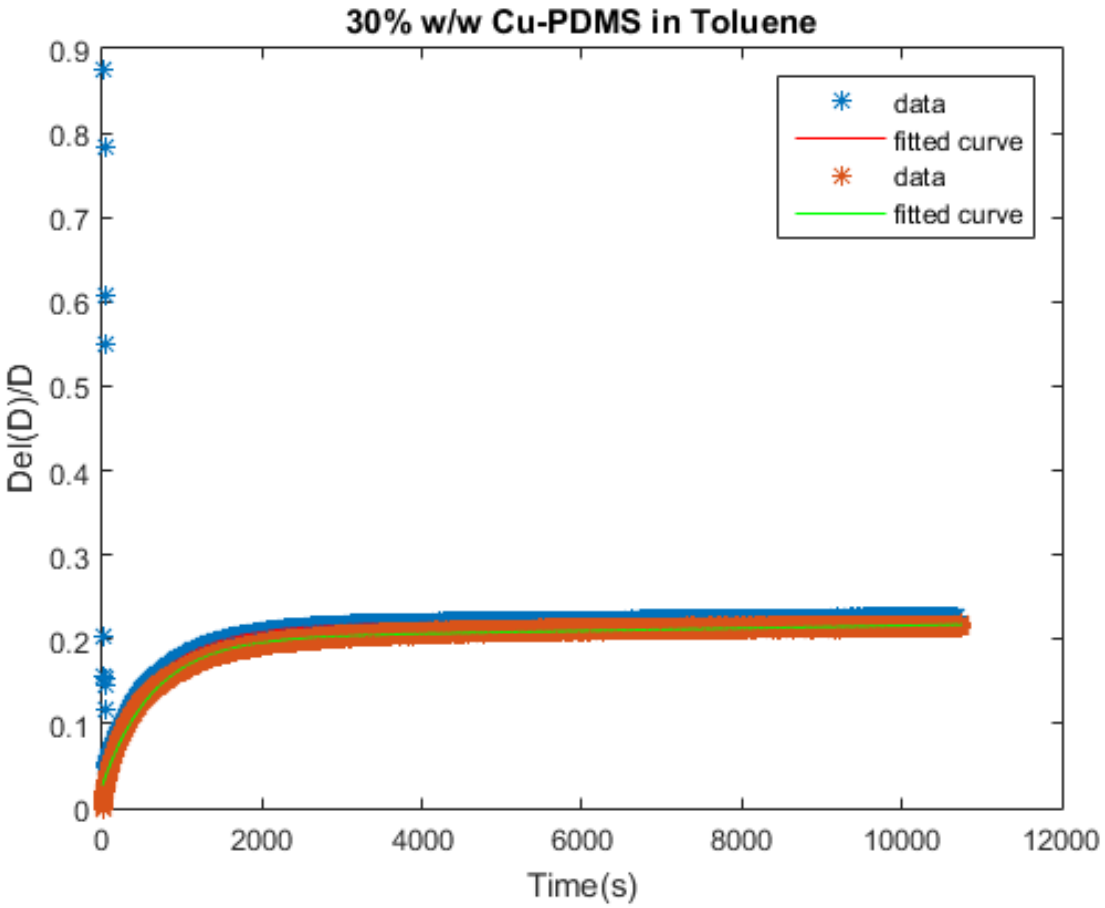

Figure 22: 30% wt. /total wt. copper composite that did not undergo the pre-curing and degassing process.

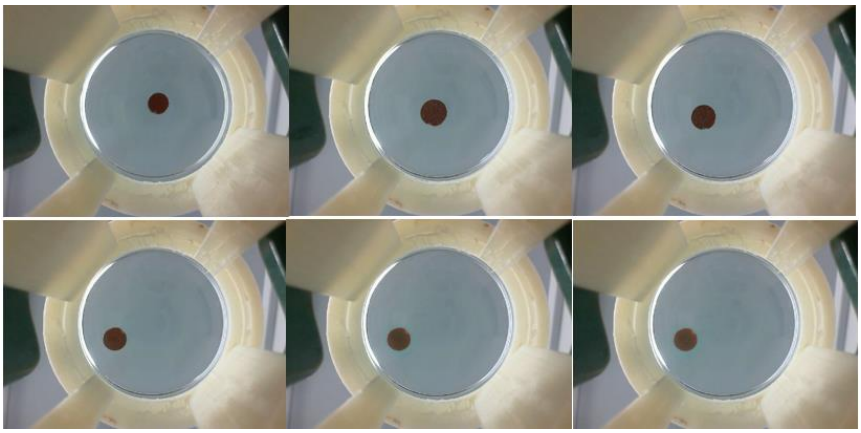

Figure 23: 30% wt. /total wt. copper particle progressively sliding off and out of the ROI.

Figure 42 shows similar discrepancies as in the figure 40. The data outlaying data occurred because the composite slide out of the ROI. Though it was caught early enough to be fixed, the fact the composite sample would not remain in their initial position would cause more issues leading on to faulty data acquisition. Figure 43 shows how the composite sample progressively moved across the bottom of the beaker thus moving out of the ROI.

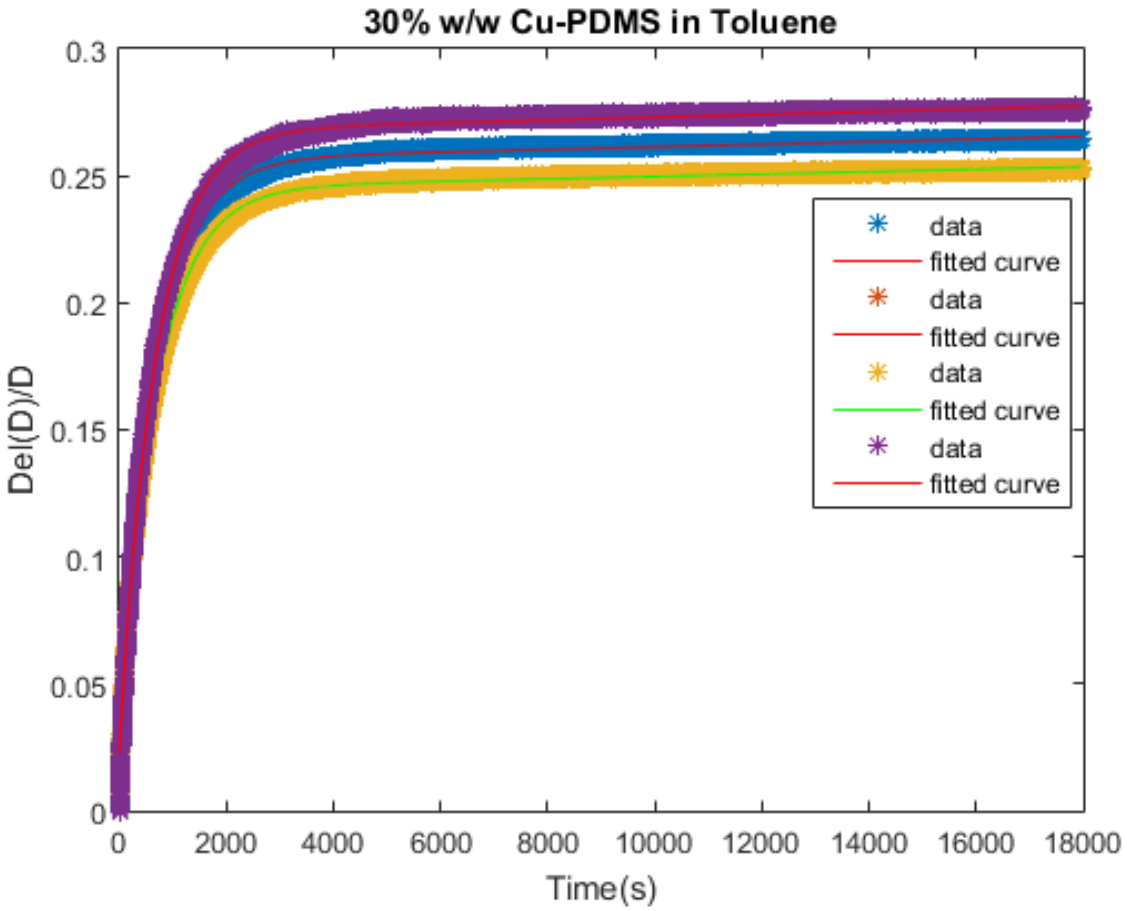

Figure 24: 30% wt. /total wt. copper composite that underwent the pre-curing and degassing process.

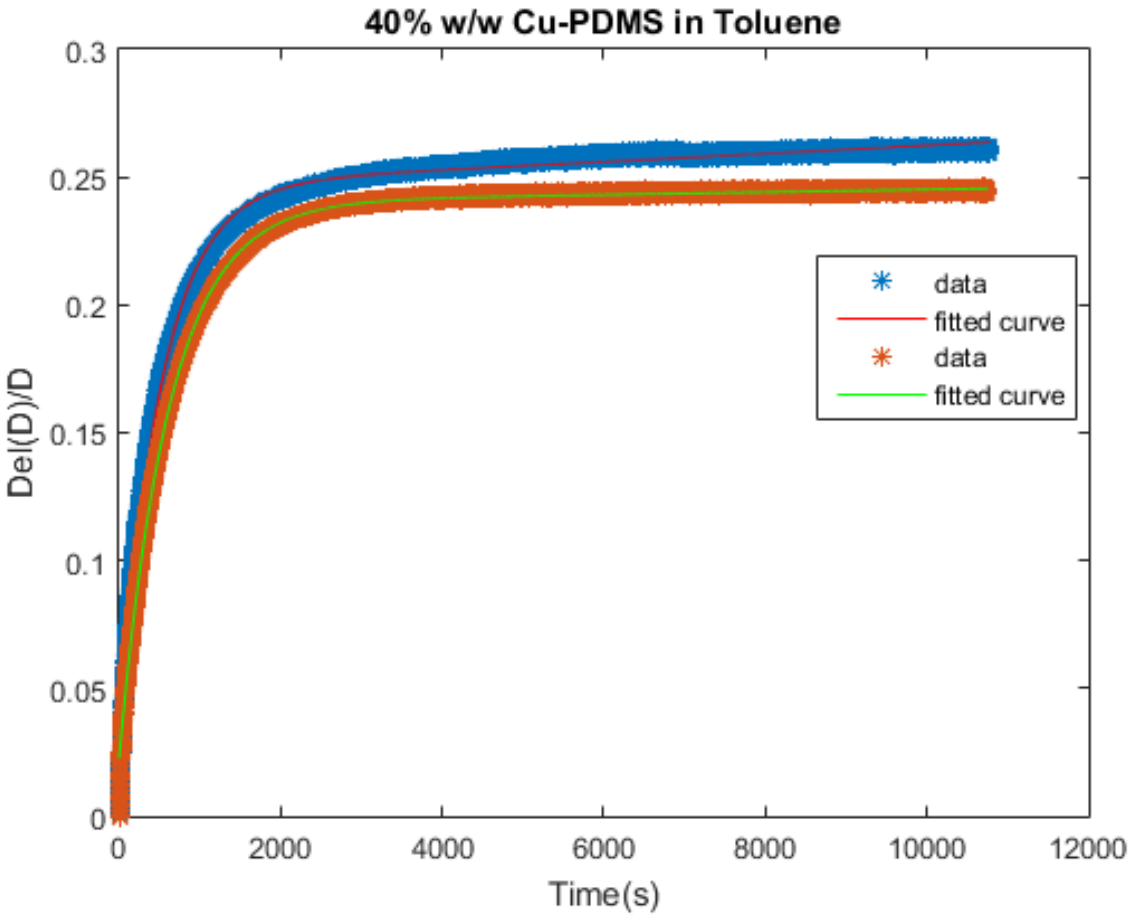

Figure 25:40% wt. /total wt. copper composite that did not undergo the pre-curing and degassing process.

As in the 20% wt. /total wt. copper composite, the 40% wt. /total wt. showed discrepancies that also highlighted the significance of the fabrication process. Two data sets were collected and plotted in Figure 26. The maximum of the blue curve is 24.67 % and the orange curve the 24.01% making a difference of about 2.67% between the two data sets. Note that the difference within the data is not as significant compared to the other data discrepancies due to the fabrication process.

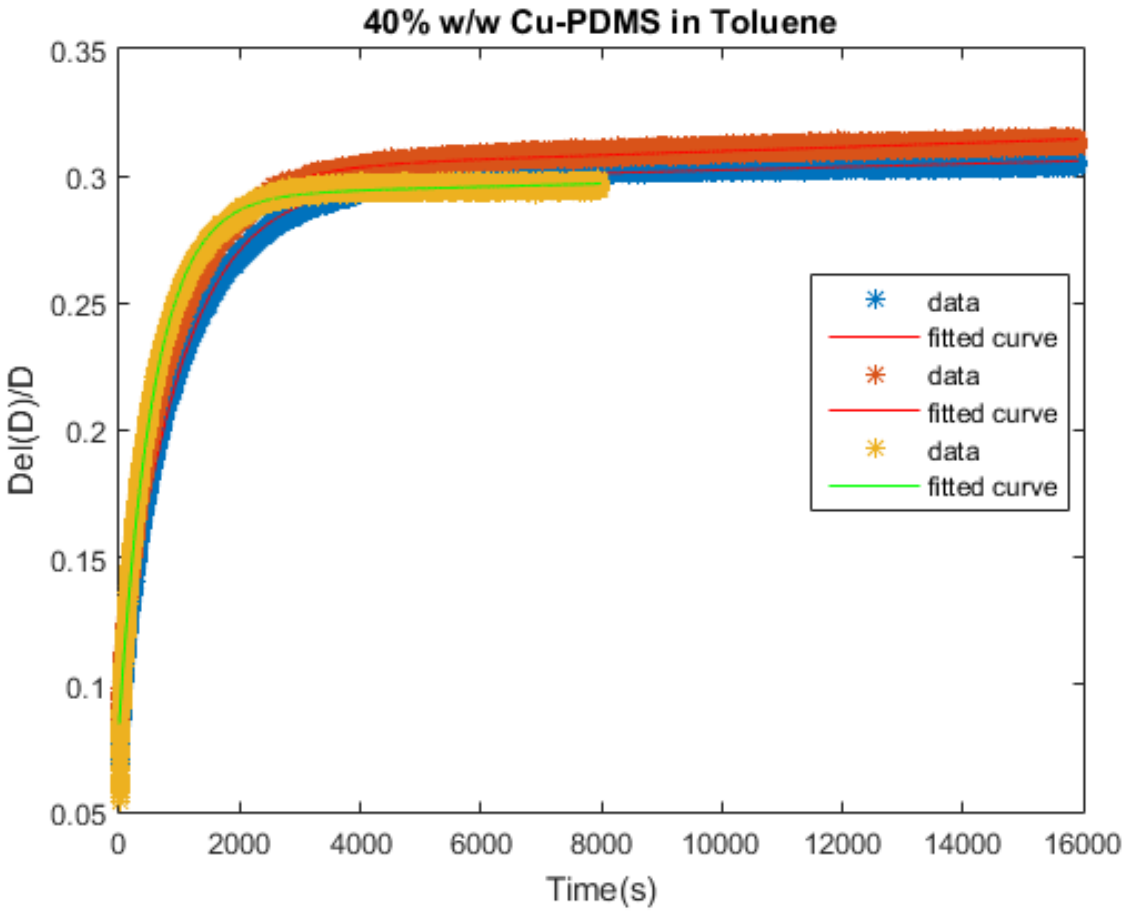

Figure 26:40% wt. /total wt. copper composite that underwent the pre-curing and degassing process.

Figure 27 shows three graph, which data from two curves were recorded for 16000 seconds and the other data set (yellow curve) was recorded for 8000 seconds. The reason for acquiring at different times lengths was simply due to the fact that the timer was set to record for those length of time for those respective curves. All three curves on Figure 46 have a maximum expansion of about 30% with a deviation of about 2%. The 40% wt. /total wt. copper composite experiment shown in Figure 46 confirmed a third time that the fabrication process is essential for obtaining uniform samples, which have a similar composition and would yield similar expansions even obtained separately. Pre-curing and degassing is an essential step for fabricating the copper-PDMS

composite samples. Omitting these steps would cause uncertainties in samples obtained from the same batch of PDMS with curing agent. Fabricating samples that would yield similar material properties is needed for running different experiments for the development process.

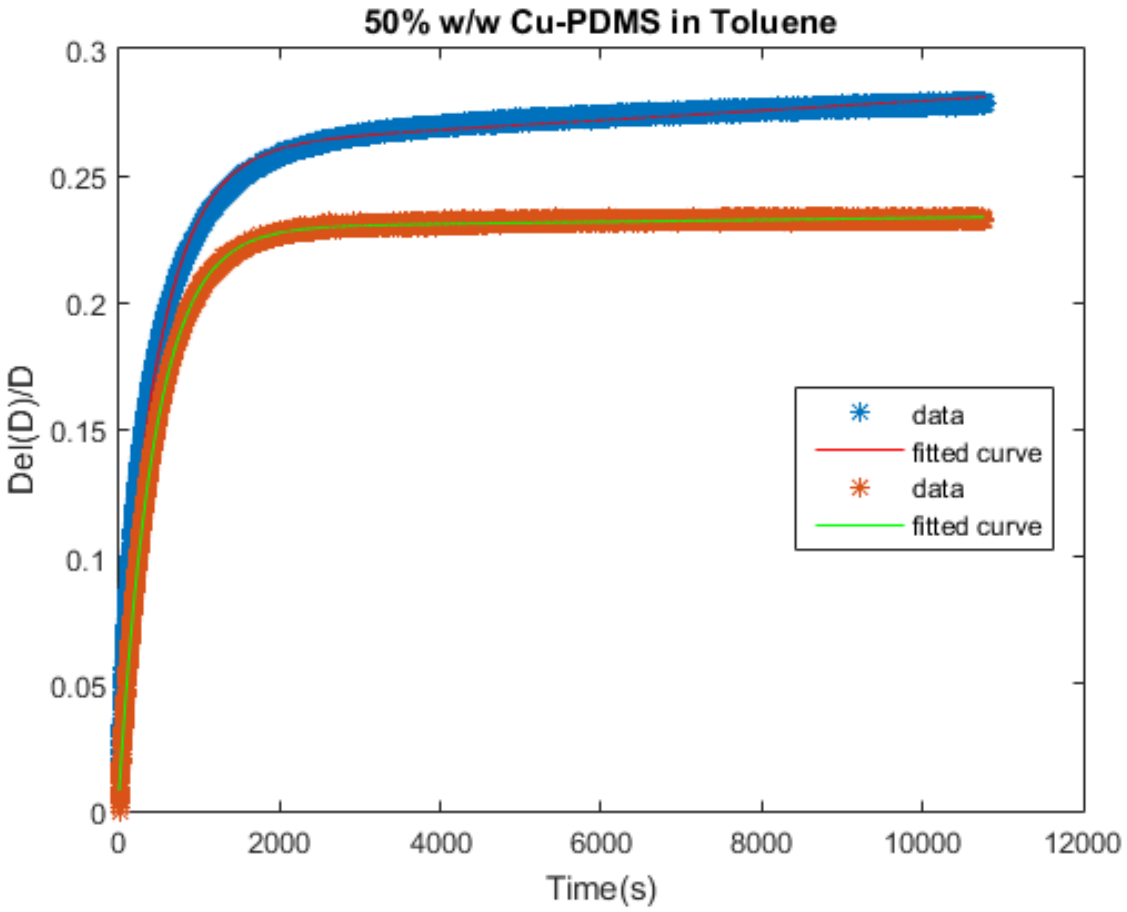

Figure 27: 50%wt. /total wt. copper composite that did **not** undergo the pre-curing and degassing process.

To contrast and clearly observe how the fabrication does actually matter, the swelling experiment was run using composite samples that had underwent the proposed fabrication process that included pre-curing and degassing (both degassing steps). The repeatability on these composite is not ideal, especially for a development procedure. The curve in blue differs between maximum

expansions by about 4%. Yet the most significant difference between both curves is the time constant which differs from one another by 75%. This is crucial parameter to have repeatable because the time constant does dictates how fast and where in the growth process the composite is. To allow a controllable etching process it imperative that the time constant and the maximum growth be precise and accurate.

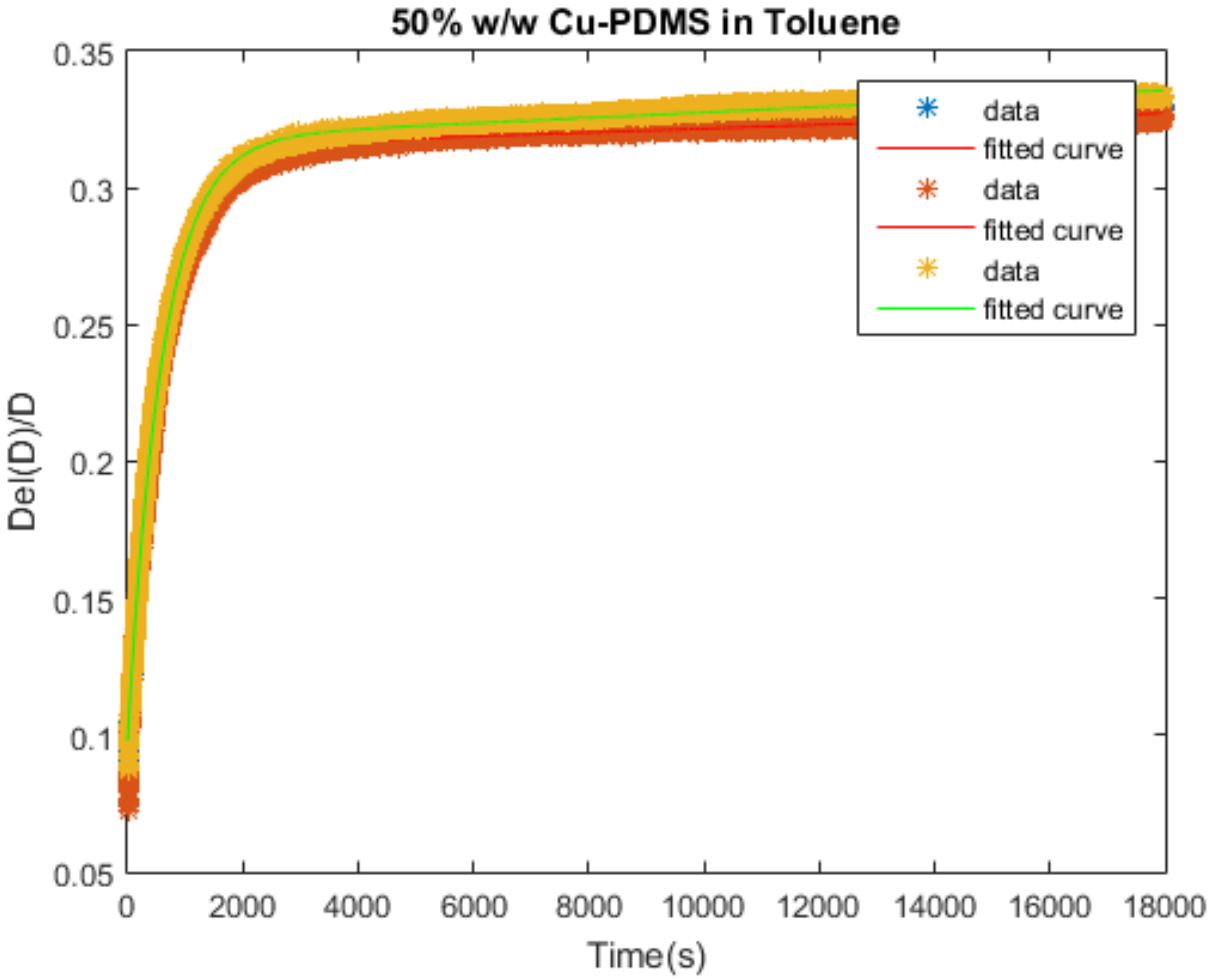

Figure 28: 50% wt. /total wt. copper composite that underwent the pre-curing and degassing process.

Chapter 5. Data and Results

1. Swelling Results of Sample in Toluene

To maintain accuracy and consistency, all results were obtained from one batch of polydimethylsiloxane, mixed with its curing agent, for samples ranging from 20% to 80%, wt. /Total wt., Copper (I) Oxide (Cu_2O) particles in PDMS (polydimethylsiloxane). Increments of 10% Weight/Total Weight Copper I Oxide particles was used to fabricate the samples and are denoted 20pCu for 20 percent Copper (I) Oxide and 80 percent polydimethylsiloxane.

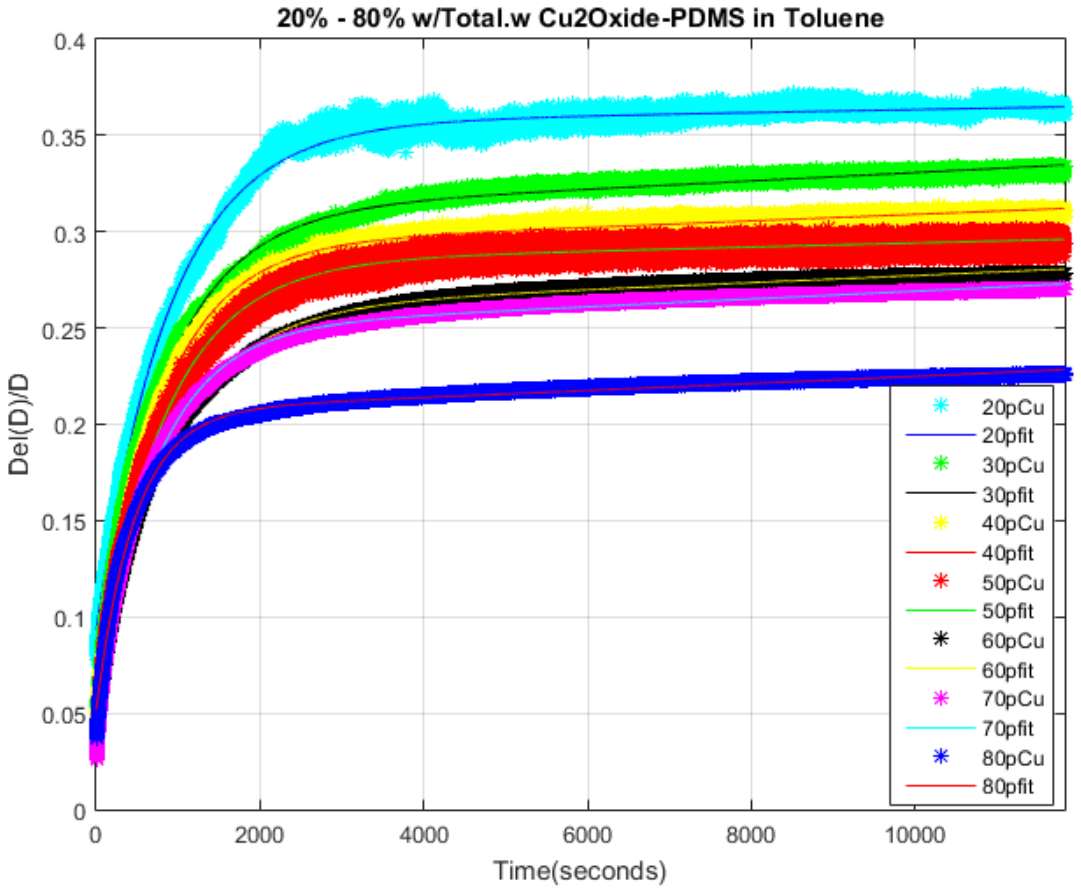

Figure 29: Over all expansion curves ranging from 20-80% wt. /total wt. copper-PDMS composites.

All samples were obtained over a period of 12000 seconds (3 hours 20 minutes) at a rate of two data per second or an interval between acquisitions of 500 milliseconds. The Microsoft LifeCam used sampled images at a rate of 30 frames per second but only two images from that series of images were processed for sizing the composite sample (15 frame intervals between processed images). A two-term exponential curve is fitted onto the data to obtain the coefficients that characterize the etching process. The fitting method is done through the Matlab® curve fitting suite. It uses a Least Square regression method to approximate a nonlinear curve fit.

$$f(s) = a * \mathrm{Exp}\left(-\frac{t}{b}\right) + c * \mathrm{Exp}\left(-\frac{t}{d}\right) \qquad (7)$$

f(s) is the nonlinear Least Square model used to curve fit the data and represents the exponential growth of the sample swelling. a is the maximum growth of the sample, b and d are the growths constants, and t is time, the independent variable.

Table 3: Two term exponential parameters for copper-PDMS composites

Weight/Total Weight	a	b - (s)	c	d - (s)
20%	0.3557	465549.3482	-0.2628	-892.0606601
30%	0.3098	153491.9417	-0.2379	-831.2551953
40%	0.2925	181719.0623	-0.2374	-755.8578987
50%	0.2839	281610.8139	-0.2203	-836.1204013
60%	0.2596	152485.5139	-0.2043	-870.3220191
70%	0.2495	131752.3057	-0.1993	-711.2375533
80%	0.2069	119817.8768	-0.1554	-469.043152

The results obtained for swelling the copper (I) oxide to PDMS composite samples are shown above in Figure 30. Table 1 above shows the parameters for 20%-80% copper (I) oxide to PDMS composite submerged in toluene only. The results obtained from experimentation show a consecutively monotonic growth of the composite samples. That is, the more PDMS there is the higher the growth is. The Figure 26 below shows the trend of maximum growth per percent copper (I) oxide composition. Although there is an obvious descending trend in the maximum growth parameter, it is noted that the trend is not uniform between percent compositions.

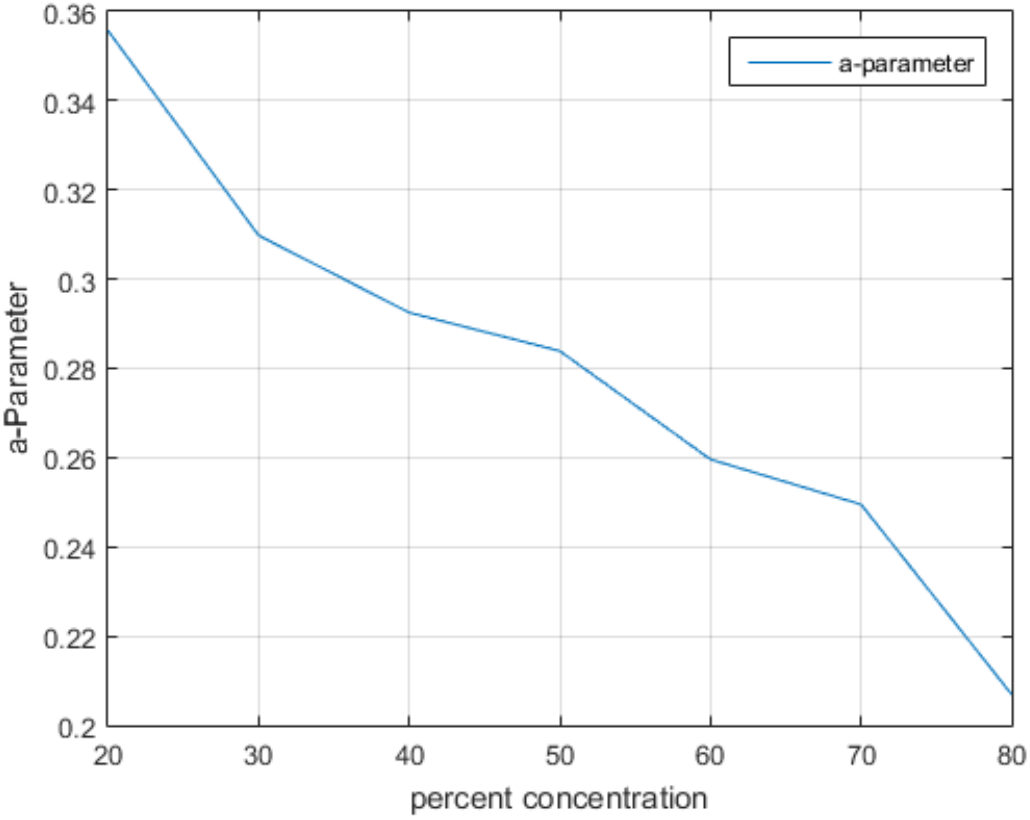

Figure 30: a-parameter progression for different composites.

Figure 27 below compares the time constants obtained for all composite samples. It is noted that all time constant fall within 34 percentile of each other except for the 20% and 50% Copper (I) Oxide. Those results show that all samples reach a relatively steady growth rate at approximately the same time. The c and d parameters are representing the secondary growth of the composite samples. Noting that c is negative for the fact that the composite sample actually shrinks over time once it has reached its maximum growth.

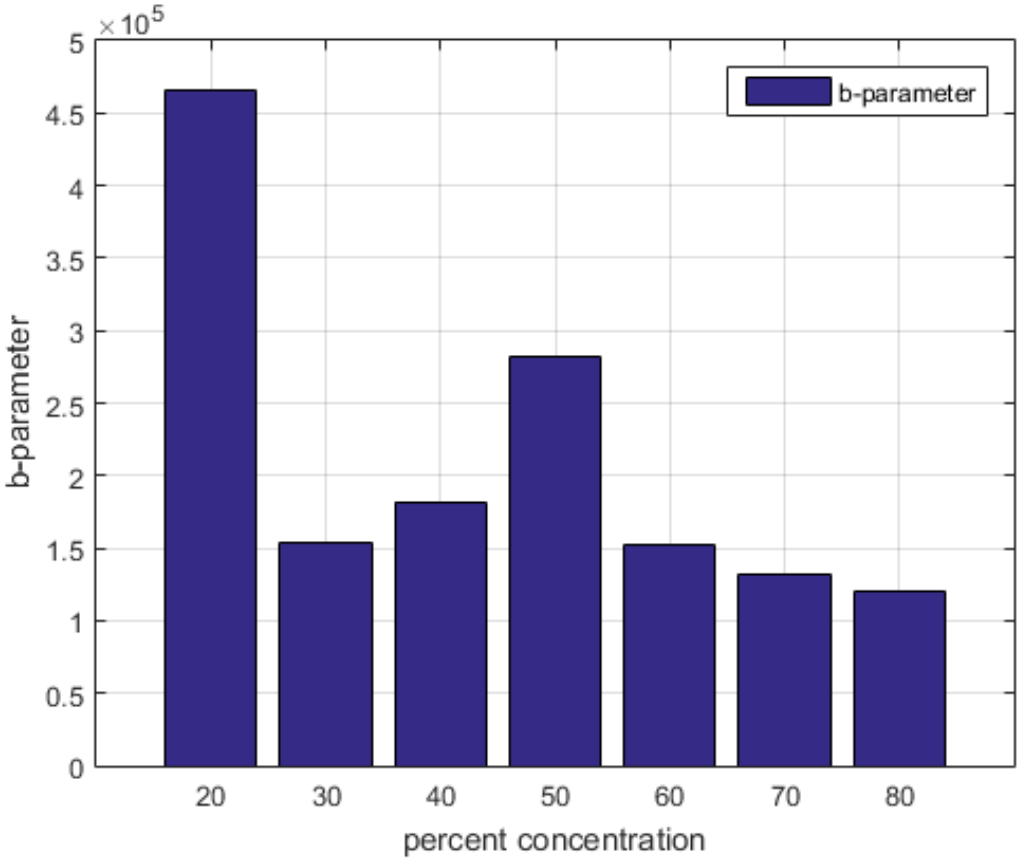

Figure 31: b-parameter progression for different composites.

2. Samples Etching Results – Acetic Acid and Toluene

Once the swelling were obtained and understood, two etching processes were used to carry out the oxide etching process. From previous research results by Pan et al. (2007). (2007), it was determined that only the 80% composite sample had the capacity to conduct current through its matrix. Although an experiment was not ran to prove that observation, it was accepted as true and used as a basis for this experiment.

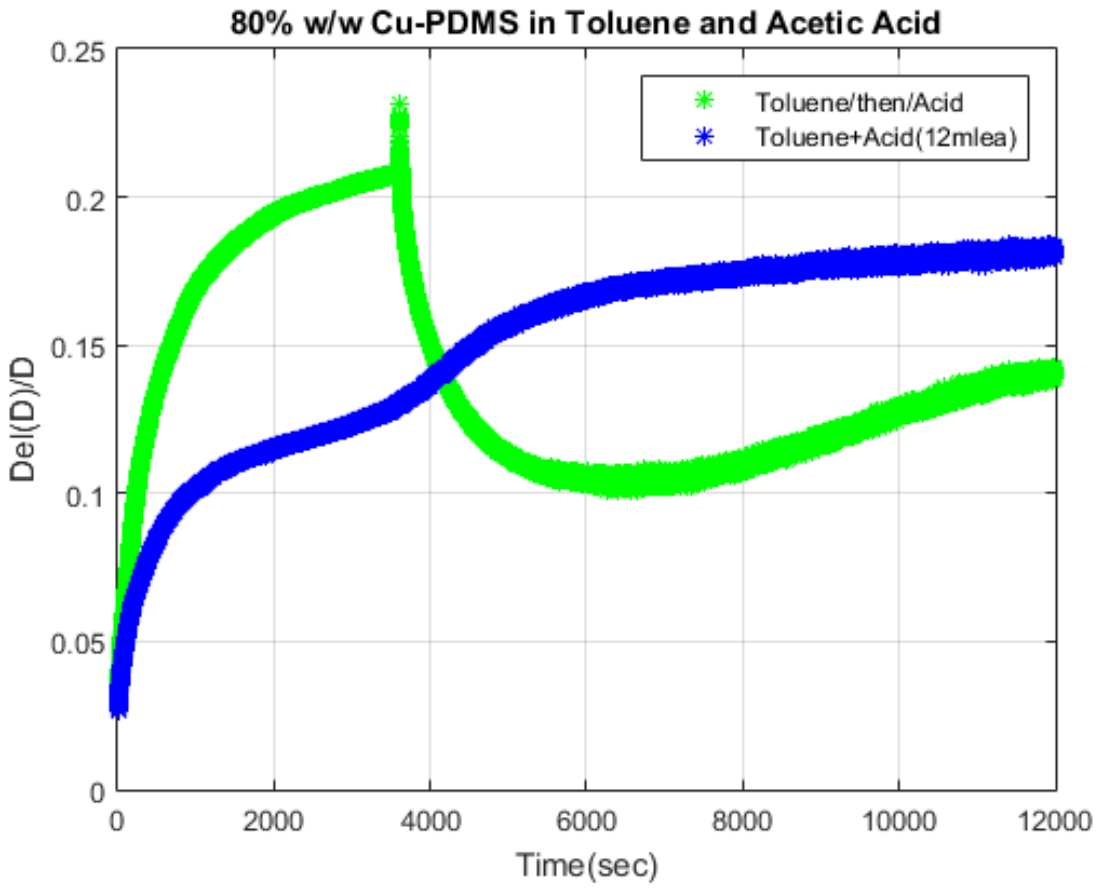

Figure 32: 80% wt. / total wt. etching curves submerged in a premixed solution and solvent (toluene) then etchant (acetic acid) solution.

The curve represented in green is the first process used for etching the oxide out of the composite sample. The sample is swollen until its known maximum growth time (~3600 seconds) then the

Acetic Acid, etchant, is added and left to etch the oxide for the remaining time (~8400 seconds). The composite sample rapidly increased to 23.17% then degraded to 10.1%, at 6564 seconds, which represents about a 50% decrease from its size prior to adding the etchant. After 12000 seconds, the composite grows up to 14.11%, which is about a 28.4% increase from the 10.1% dip. During the etching process, the Acetic Acid and Toluene bath changed from a colorless solution to a blue like color showing signs of ionized copper presence in the solution.

Figure 33: Ionized oxygen, toluene, and acetic acid solution.

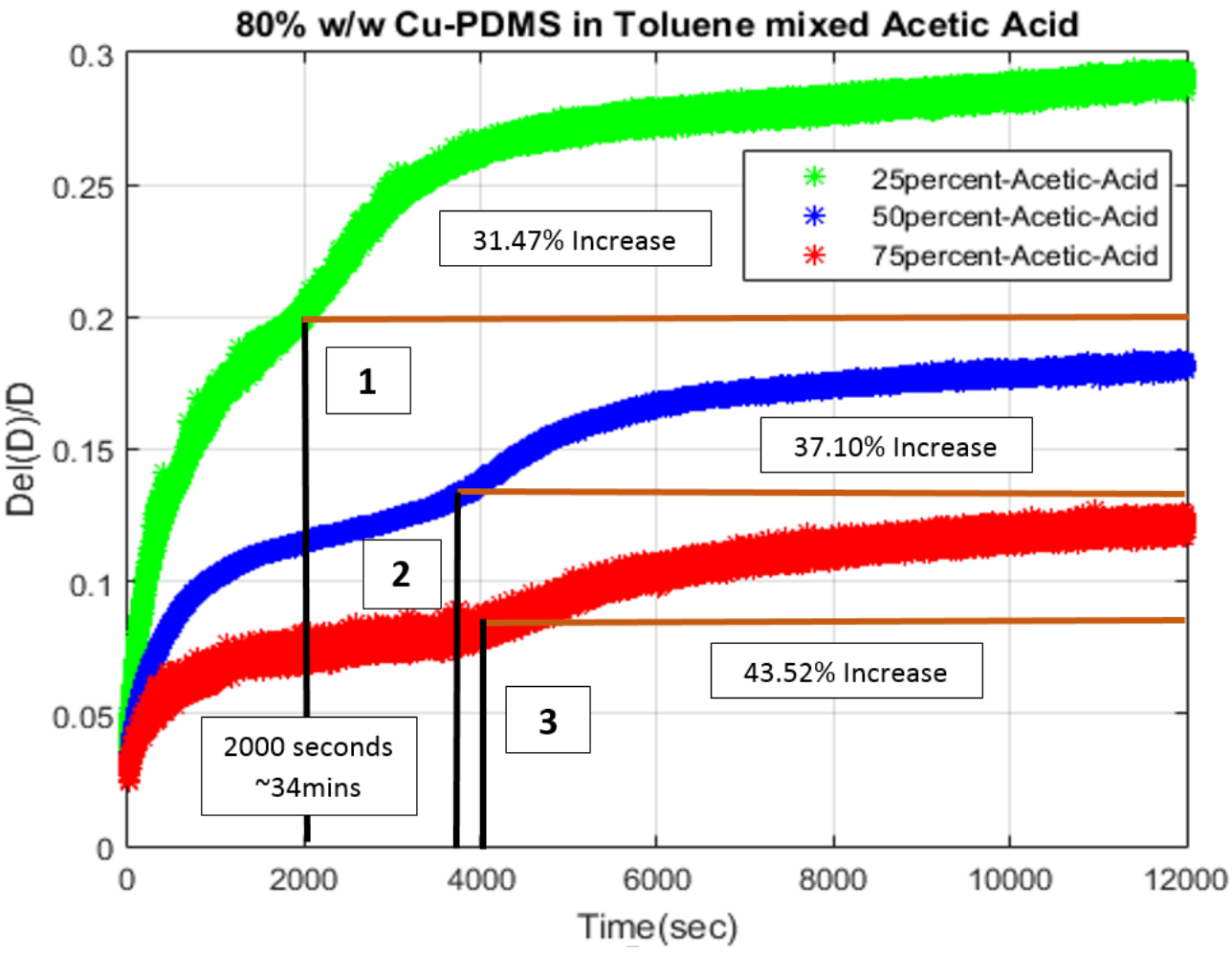

Figure 34: Second expansion instance investigation curves.

It is also noticed that if the composite sample is left in the bath for several hours post experiment, a layer of oxide forms on top of the sample. This phenomenon has only been observed on certain composite samples without any conclusive patterns. The second etching process used to remove the oxide from the 80% composite sample consists of premixing the Toluene and the Acetic Acid and plunging the composite sample in that solution for 12000 seconds uninterrupted (blue curve in figure 30). Due to the fact that two growth instances were observed in the solution of 12ml Toluene and 12ml Acetic Acid, 50% volume percent Acetic Acid mixture, more data were recorded at 25% V/V Acetic Acid mixture, and 75% V/V Acetic Acid mixture, as seen in figure

35. Three different solution mixtures used to swell the 80% composite sample are shown above in figure 35. For all three solutions, two distinct swelling instances are observable. In the 75% V/V Acetic Acid mixture (1st Box), the composite sample saw a boost, in its growth, of 43.52% in the second instance; the 50% V/V Acetic Acid mixture (2nd Box) a boost of 37.10%; and the 25% V/V Acetic Acid mixture (3rd Box) a boost of 31.47%. The boost seen in the growth of the composite is directly proportional to the amount of Acetic Acid present in the solution. The higher the percent content of Acetic Acid there is in the solution, the higher the composite sample increases. This may be relative to the amount of oxide removed from the composite sample thus exposing polymeric surfaces accessible to the swelling agent, toluene. Once the time allocated for etching has passed, the composite samples initially dark brown changes into a light reddish color. This shows that the oxide, once present in the matrix on the polymer, has now been removed. Quantifying the amount of oxide is yet to be experimented. The pictures shown below are those obtained from the 80% composite sample in the 50% V/V Acetic Acid and 75% V/V Acetic Acid mixtures. Though obvious that the color has changed and that it is a sign of oxide removed, there is more accurate method of quantifying the amount of oxide removed that may be used in the future.

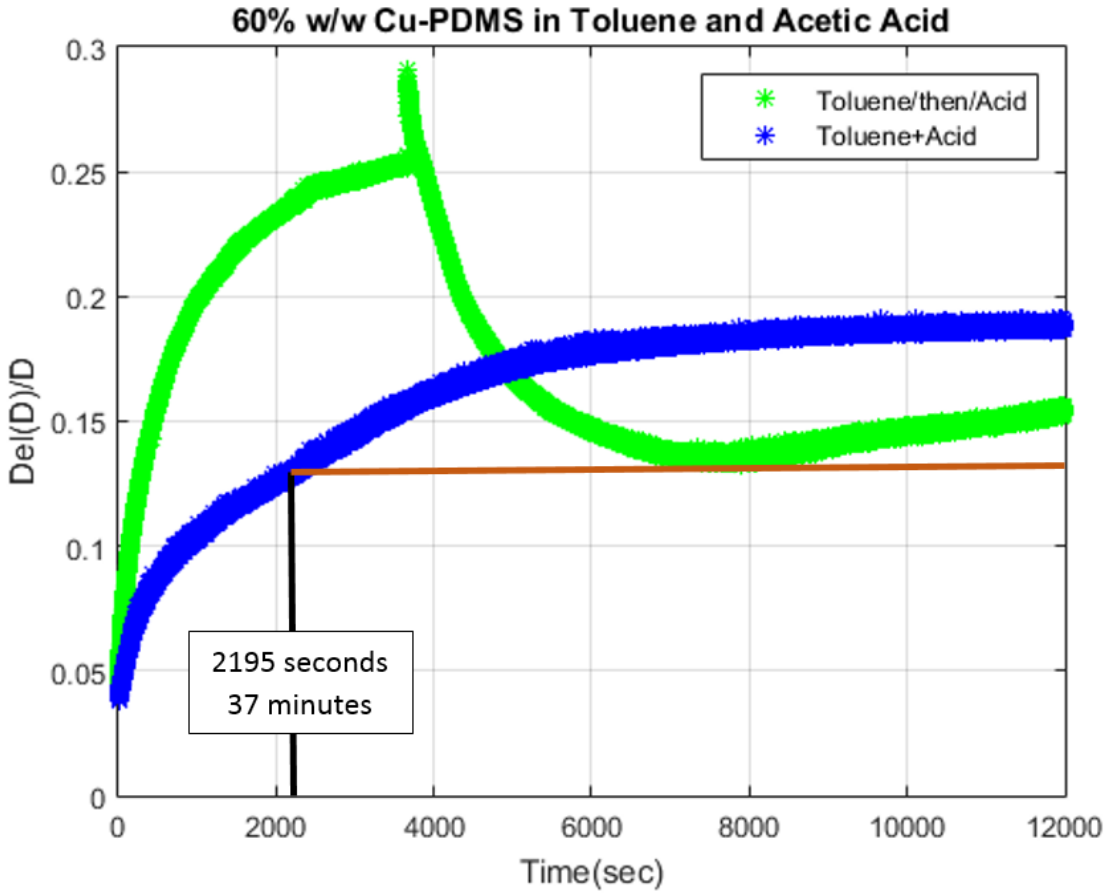

Figure 35: 60% wt. /total wt. copper composite samples in pre-mixed toluene and acetic acid and toluene then acetic acid.

A 60% composite sample was also taken through the same process as the 80% composite sample. At first, the composite sample was left to grow in Toluene for ~3600 seconds then the Acetic Acid was added to the beaker. The composite sample remained in that solution for the remainder of the time, ~8400 seconds. The composite sample rapidly increased to 29.06% then degraded to 13.30% at 7736 seconds, which represents about a 64% decrease from its size prior to adding the etchant. After 12000 seconds, the composite grows up to 15.43%, which is about a 13.80% increase from the 13.3% dip. During the etching process, the Acetic Acid and Toluene bath changed from a colorless solution to a blue like color showing signs of ionized oxygen presence in the solution

just as observed in the 80% composite sample. The second etching process used to remove the oxide from the 60% composite sample is similar to the one used for the 80% composite samples and consists of premixing the Toluene and the Acetic Acid and plunging the composite sample in that solution for 12000 seconds uninterrupted (blue curve in figure 36).

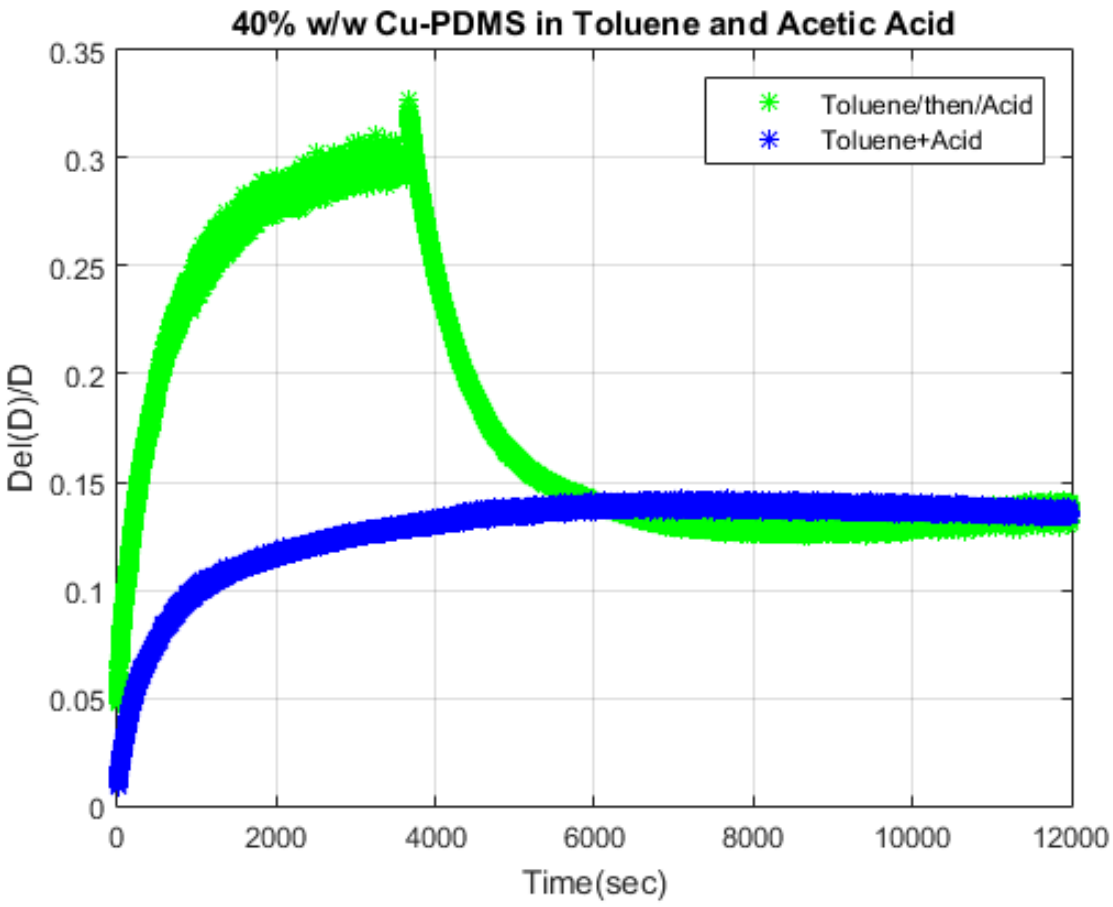

Figure 36: 40% wt. /total wt. copper composite samples in pre-mixed toluene and acetic acid and toluene then acetic acid.

Just like the 80% composite samples, two growing instances are observable on the composite sample. A 31.72% increase was observed at 2195 seconds, where the composite sample had grown 12.83%, to 12000 seconds, where the sample had grown 18.79% (also is the final

recorded size of the 60% composite sample). The 40% and 20% composite samples were also experimented for removing the oxide from the Copper (I) oxide particles embedded in the PDMS matrix. Similar processes were carried out where in process one - the etchant is added after the composite samples had attained there maximum growth size, and in process two – the Toluene and Acetic Acid (etchant) are premixed and the composite sample grown in that mixture the entire time. The graphs obtained below (figure 35 and 36) are plots of the data resulting from the experiment.

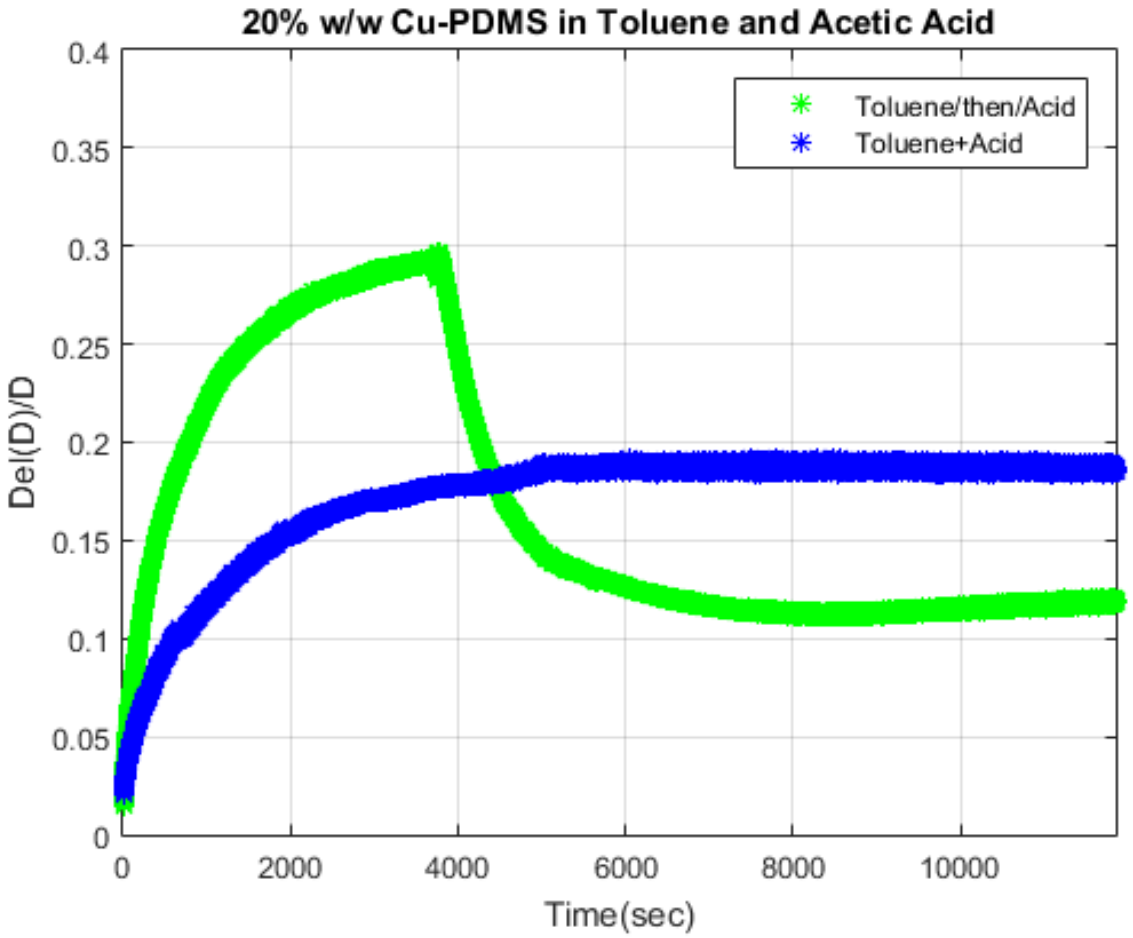

Figure 37: 20% wt. /total wt. copper composite samples in pre-mixed toluene and acetic acid and toluene then acetic acid.

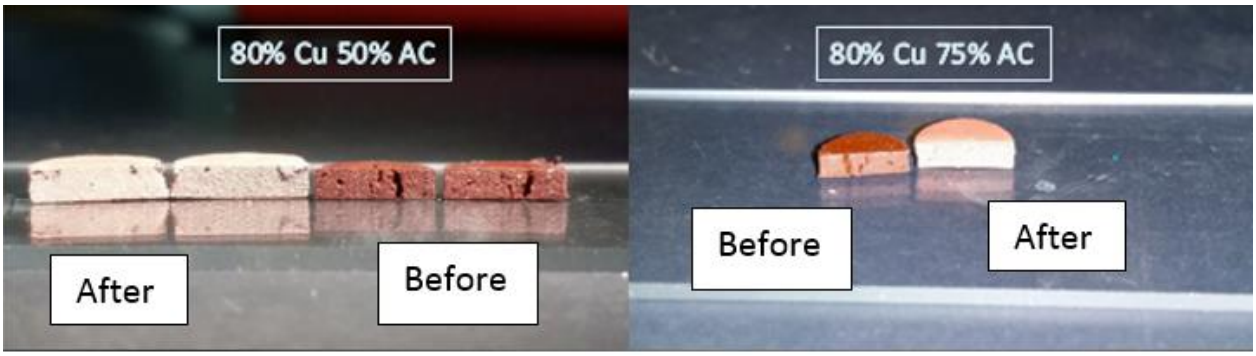

Figure 38: Before and after 80% wt. /total wt. in 50% acetic acid and toluene and 75% acetic acid and toluene solutions.

3. Fabrication Effects on Results

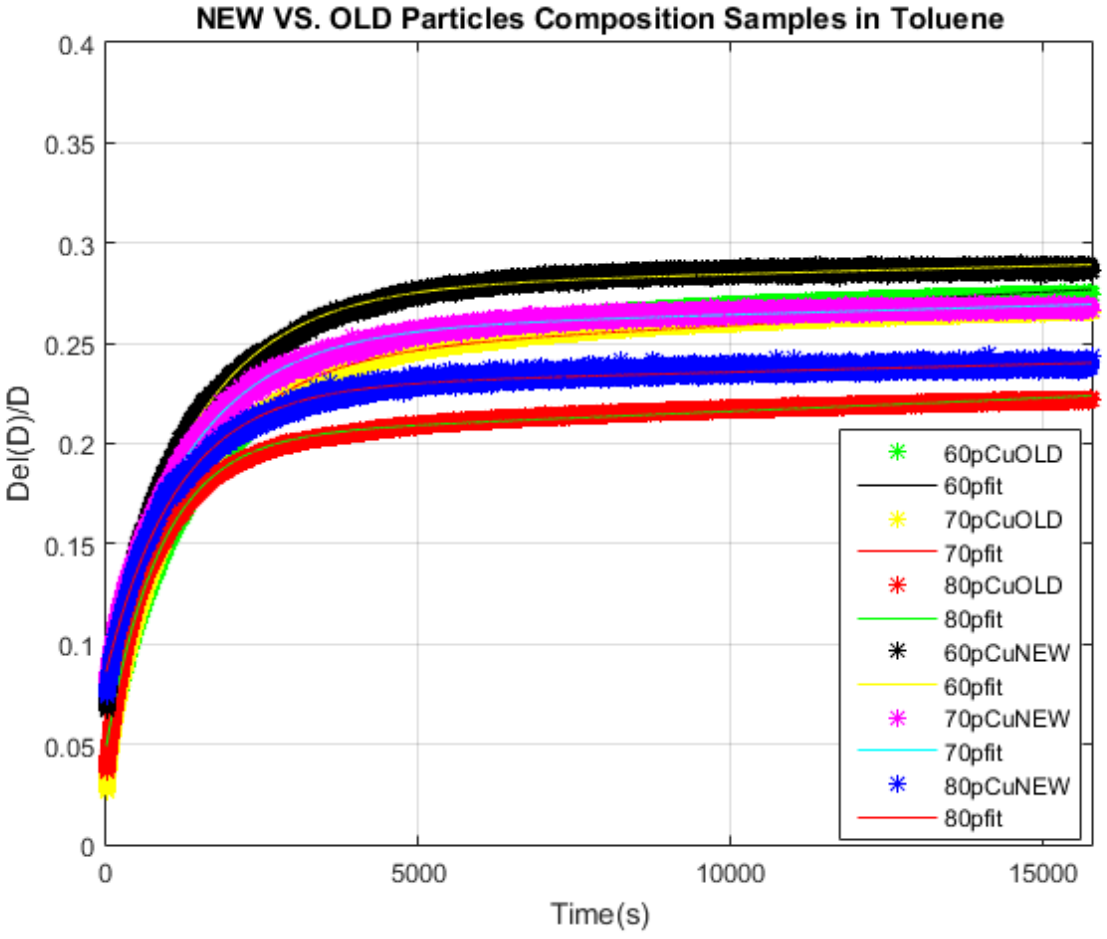

Figure 39: New versus old copper particles composite samples in toluene only.

Table 4: Parameters for new versus old copper particles composite samples in toluene only.

	Weight/Total Weight	a	b - (s)	c	d - (s)
OLD	60%	0.2524	170328.7345	-0.2003	-1599.744041
	70%	0.2432	159235.6688	-0.19965	-1309.243257
	80%	0.2033	164257.5558	-0.1544	-871.8395815
NEW	60%	0.2767	356252.2266	-0.1899	-1384.466288
	70%	0.2558	305157.1559	-0.1625	-1367.989056
	80%	0.2278	295683.0278	-0.1417	-1128.413451

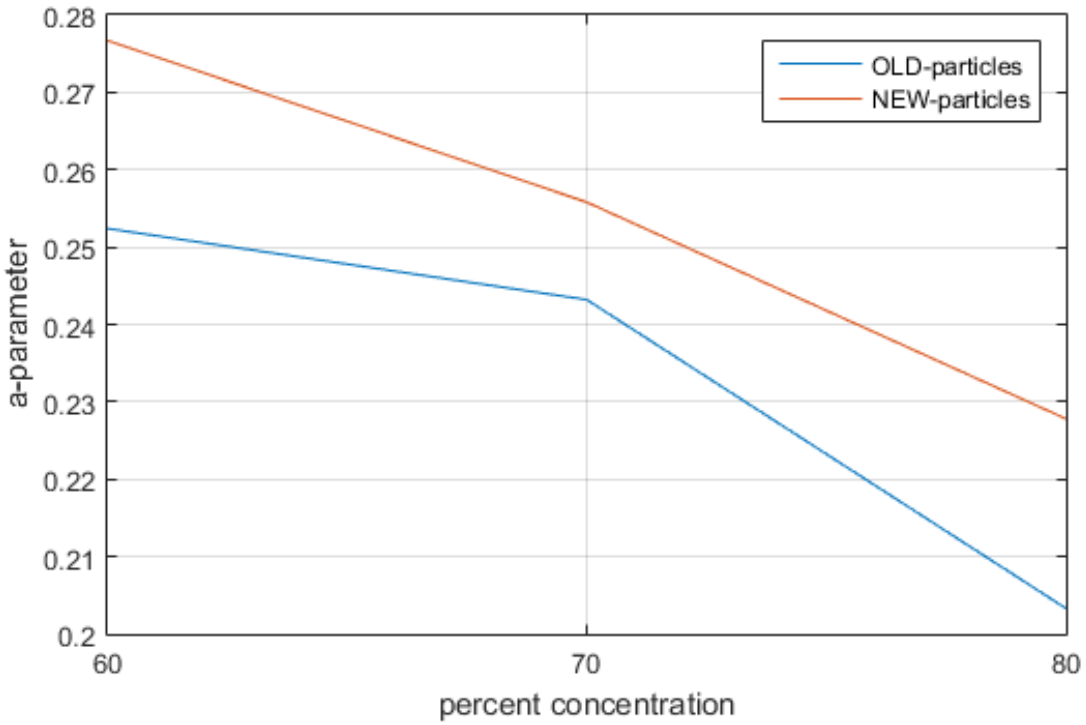

Figure 40: a-parameter of the new and old copper particles. New being the copper particle with no oxide layer and old being the copper (I) oxide.

The fabrication process noticeably affected the results obtained. Several fabrication parameters affect the homogeneity, the materials elasticity (this is assumed due to the variability in growth from one batch to the other of supposedly similar composite samples), and oxide content of the composite samples. Two batches of Copper (I) Oxide were experimented on for a better understand of the effects that the oxide content has on the swelling and etching processes. Table 2 gathers the parameters obtained from curve fitting the data collected from the new copper particles and the old copper particles.

The 60% Copper (I) Oxide new particles composite sample differed from the old particles composite sample by 2.43%; the 70% Copper (I) Oxide new particles differed by 1.26%; and the 80% Copper (I) Oxide differed by 2.45%. These results show that all three percent compositions differed by at least 1%. These results are shown in Figure… as well for clarity between the differences of a – parameters obtained.

Unlike the old 80% Copper (I) Oxide composite sample, the new 80% Copper (I) Oxide composite sample converged to a similar size for both etching processes. Both processes expanded and etched the composite sample to 18.30% at the end of the data acquisition period. Most importantly, there is no second instance noticeable on the process where both the etchant and the swelling agent are premixed. The expansion of the composite sample is fairly constant and undisturbed until its steady state swelling size. This observation clearly adds to proving the hypothesis drawn to states that the amount of oxide contained on the native copper particle dictates how much does the composite sample grows.

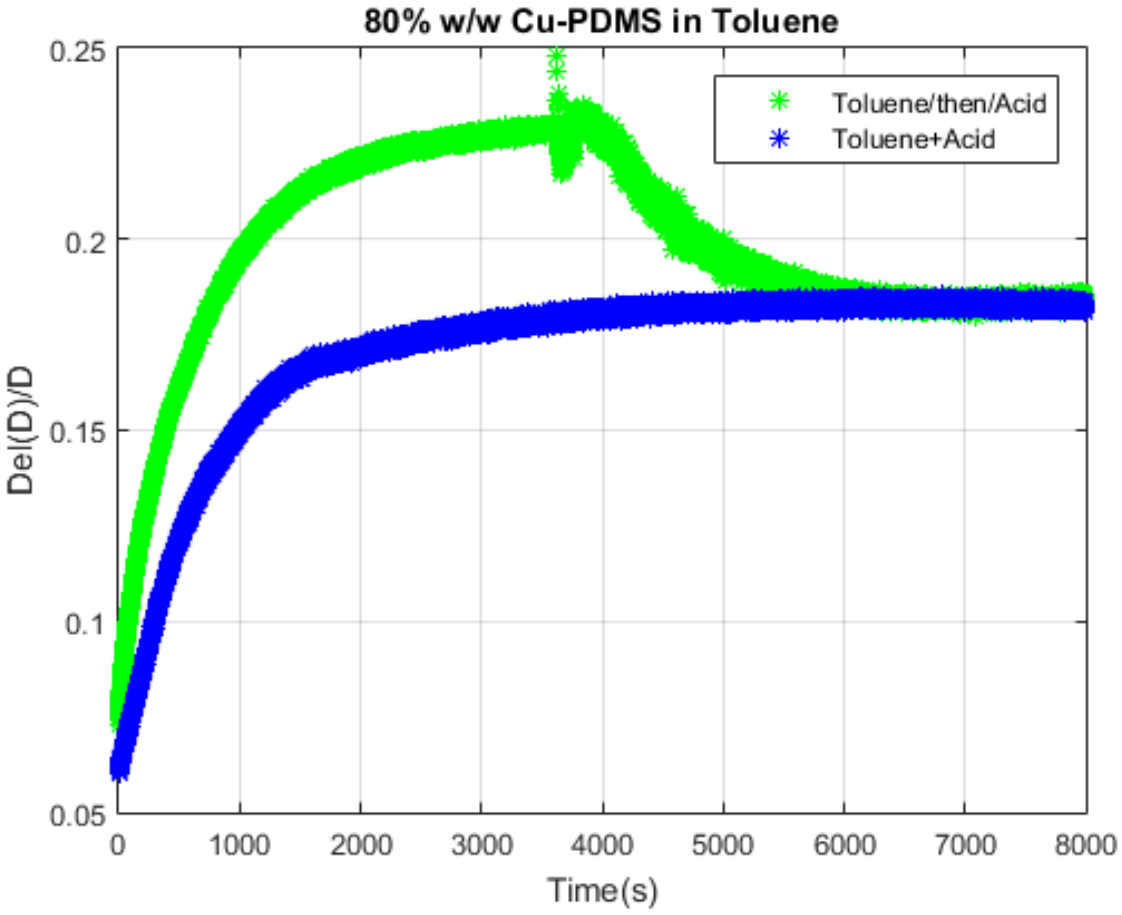

Figure 41: New copper (I) particle 80% wt. / total wt. etching curves submerged in a premixed solution and solvent (toluene) then etchant (acetic acid) solution.

That proof is reiterated below in figure 38 where both etching processes converge to a final size of 15.7% and 14.3% for a difference of 1.4%. As a result, it is now understood that the quality of the Copper (I) Oxide particles does affect the swelling and etching process. The solution in which the sample is submerged for etching the oxide is also important and dictates the time it takes to remove the oxide off of the native copper particles. It is has been validated that the more swelling agent there is in the solution the faster the etching process occurs, up 1800 seconds faster than the closest known mixture.

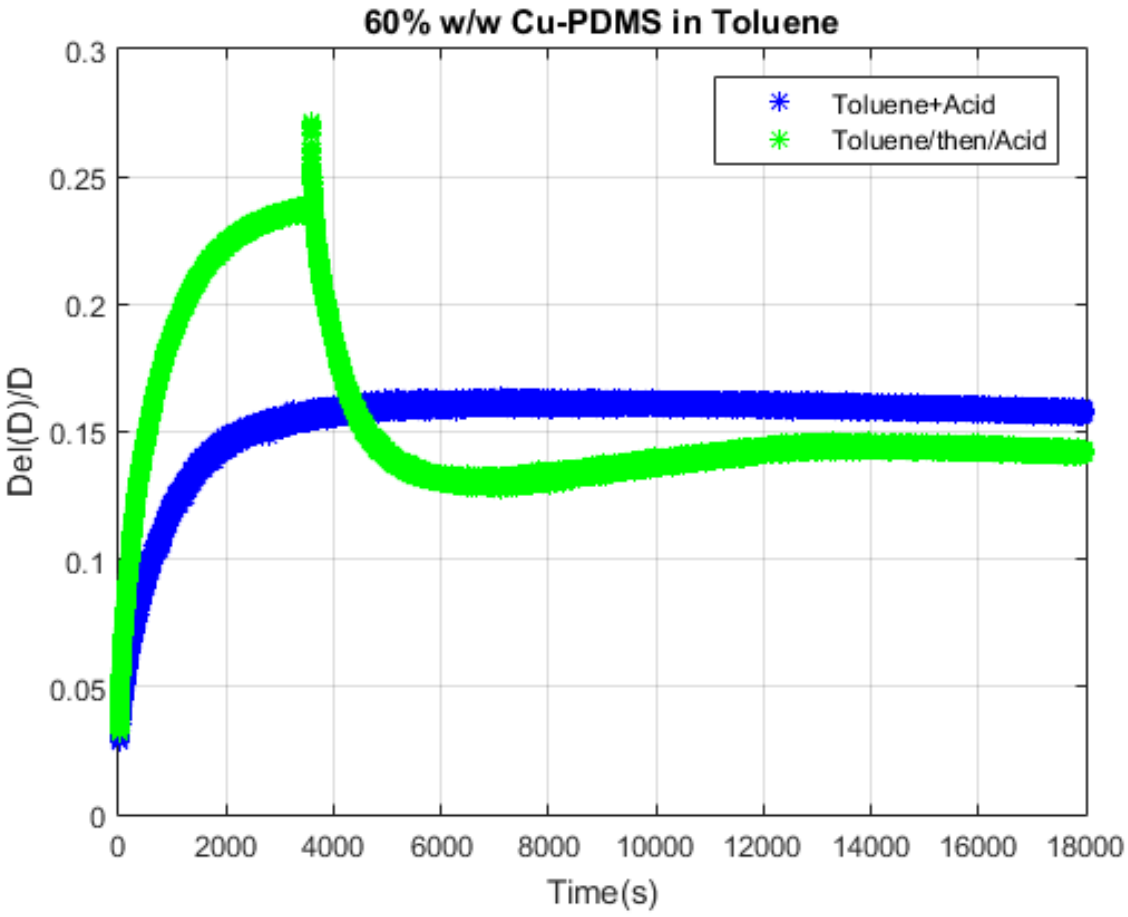

Figure 42: New copper (I) particle 60% wt. / total wt. etching curves submerged in a premixed solution and solvent (toluene) then etchant (acetic acid) solution.

Chapter 6: Conclusion

This thesis attempted to answer several questions regarding the development of a novel corrosion sensing technique. Pan et al. (2007)'s research gave the preliminary research results essential for developing the etching process and obtaining essential parameters for the composite sample fabrication process. The swelling data, where the composite samples were submerged and left to grow in Toluene, are consistent and concurrent with previously reported data. Several fabrication criterion were deduced to have some effect on the growth of the composite sample. It was concluded that a consistent batch of PDMS mattered for a repeatable and stable data acquisition. Variations of pure PDMS 10:1 ratio would differ from one batch to the other. It is essential to know that the amount of curing agent does in fact cause the polymer to solidify more or less depending on the excess quantity of curing agent. The quality of copper (I) oxide particles used also affected the b - time constants parameter of the composite samples (60%, 70%, and 80% composite particles). It was deduced that the less oxide there is on the particles used to make the composite samples, the more it grew (hint the higher the maximum expansion) and the faster it reached its maximum growth size. The 60% copper (I) oxide new particles composite sample differed from the old particles composite sample by 2.43%; the 70% copper (I) oxide new particles differed by 1.26%; and the 80% copper (I) oxide differed by 2.45%. These results show that all three percent compositions differed by at least 1%. These results align with the concluded fact that the oxide formed on the copper particles prohibits the swelling agent from swelling the composite samples. This conclusion is again demonstrated while etching the oxide from the copper (I) oxide particles embedded in the PDMS matrix. It is demonstrated in Figure 36, in the data and results chapter 5, that the less Toluene there is in the etching/swelling solution, the longer it took for the etchant to remove the oxide. The highest growth was seen on the 25% V/V Acetic Acid where the

solvent was 75% V/V of the total volume of the solution. The second growth instance seen on Figure 36 occurred at 1800 seconds or 30 minutes faster than the 50% V/V Acetic Acid solution. This is deduced to be the most effective oxide etching process where it is understood that more solvent allows the etchant to flow through the PDMS matrix to attack and etch the oxide off of the native copper particles. The more etching percentage there is in the solution the less likely it is to flow through the densely packed PDMS matrix. The pre-curing and degassing steps also were observed to affect the quality of the data obtained. It was shown that the pre-curing step does in fact allow the copper (I) oxide particle to remain suspended in the PDMS mixture. Otherwise the copper (I) oxide particles would settle down to the bottom of the mixture causing the cured samples to have non-uniform physical properties. The degassing process is also essential because it reduced the amount of air pockets locked into the copper (I) oxide to PDMS mixture. Both steps were proven essential for obtaining consistent and repeatable data.

In summary:

a. The oxide removal process was successfully carried out.

b. The level of de-oxidization could potentially be predicted with further experimentation.

c. The more toluene there is in the toluene-acetic acid solution, the faster the second instance occurs.

d. Also premixing toluene and acetic acid before submerging the composite samples is a faster oxide removal process than the other by about half the time.

e. Oxide free copper particles (New particles) composite samples exhibit similar expansion behaviors as copper (I) oxide particles composite samples when submerged in toluene only.

f. Preliminary data recorded emphasized the importance of the pre-degasing step and the pre-curing step for particle homogeneity in the composite samples.

g. The estimated cost for fabricating a sensing device is less than € 50

Future Work

This thesis carried on the work of Pan et al. (2007) on parameterizing and characterizing the fabrication of the corrosion monitoring sensing material composed of copper (I) oxide particles and polydimethylsiloxane. A major future work consists of investigating the etching process of other metals as done by Pan et al. (2007) of their metal particles to PDMS composites. A significant aspect of the fabrication process is the size effect of the sample on the etching process. Pan et al. (2007) dissertation and this thesis characterized a 6.35 mm x 1 mm samples only. A clear understanding of the size effect on the etching speed and solution concentration needed would be a great addition to understanding the novel corrosion sensing material best functional size. Once the etching process and size effect are well understood, the impedance of the composite sample will need to be investigated for ideal sensing capability. A stable impedance reading must be sought which would allow a clear and concise impedance variation over time. The understanding of time variation of the impedance will lead to properly sizing the sensing material for the rate of oxidization desired and the sensing life of the sensing material.

References

1. F. Pan, Abdoul Kader Maiga, and A. Huang. *Solvent-Based Polymer Swelling Characterization For the Developement fo the Nano/Micro-Particle Polymer Composite MEMS Corrosion Sensor.* Montreal, Canada : ASME Proceedings, 2014.

2. Doctors, Corrosion. Silver Bridge Collapse. *Corrosion Doctors.* [Online] April 17, 2015. http://corrosion-doctors.org/Bridges/Silver-Bridge.htm.

3. Corrosion Managment. *Rohrback Cosasco Systems.* [Online] Rohrback Cosasco Systems. [Cited: April 17, 2015.] http://www.cosasco.com/products-c-396-l-en.html.

4. *Prediction and real-time monitoring techniques for corrosion characterisation in furnaces.* Linjewile Temi M., et al., et al. 2, s.l. : Material at High Temperatures, 2003, Vol. 20.

5. *2009 Frank Newman Speller Award Lecture: Prevention and Control of Corrosion in Aircraft Components-Changes Over Four Decades.* Hinton, B. 8, Houston : National Association of Corrosion Engineering, 2010, Vol. 66.

6. *A Novel Method of Etching Copper Oxide Using Acetic Acid.* K.L.Chavez, D.W Hess. 11, s.l. : Journal of Electrochemical Society, 2001, Vol. 148.

7. Pan, Fen. *DEVELOPMENT OF MEMS-BASED CORROSION SENSOR.* Fayetteville : University Arkansas, 2010.

8. Additives, Joint Expert Committee for Food. *Polydimetholsiloxane.* s.l. : Family Nutritional Program, 2003.

9. Category Archives: Grayscale. *Letters on Design.* [Online] February 2014. [Cited: April 29, 2015.] http://lettersondesign.com/category/grayscale.

10. Color Representation. *Colgate.edu.* [Online] [Cited: May 06, 2015.] http://cs.colgate.edu/~chris/cs122web/Unit%201%20P.E/Color%20Representations.html.

11. Tang. *Cross-Linked PDMS Expansion due to Submersion in Liquid and Supercritical CO2.* Fayetteville : Unoversity of Arkansas, 2012.

12. Roberge. *Handbook of Corrsion Engineering.* New York : McGraw-Hill, 2000.

13. N. Lee, C. Park, and G. M. Whitesides. *Solvent Compatibility of Poly(dimethylsiloxane)-Based MicroFluidics Devices.* s.l. : Analitycal Chemistry, 2003.

14. Jones, D. A. *Principles and Prevention of Corrosion.* New Jersey : Upper Saddle River, 1996.

15. G. Ruschau, S. Yoshikawa, and R. Newham. *Percolation Constraints in the Use of Conductor-Filled Polymers for interconnects.* s.l. : IEEE Proceedings, 1992.

16. F. Pan, J. lee, A. D. S. Jones and A. Huang. *Improved Micro Patterning of Soft-Polymers and Elastomers Using Comformally Coated Omni Coat Nanofilms.* s.l. : ASME Proceedings (Micro and Nano Systems), 2008.

17. A. Huang, V. T. S. Wong and C. M. Ho. *Silicone Polymer Chemical Vapor Sensors Fabricated by Direct Polymer Patterning on Substrate Technique.* s.l. : Sensors and Actuators (B Chemical), 2006.

18. *A Theoy on Cathodic Protection.* R. B. MEARS, R. H. BROWN. Rochester, N.Y. : Electronic and Photonic Devices, 1938. 519-531.

Appendix 1

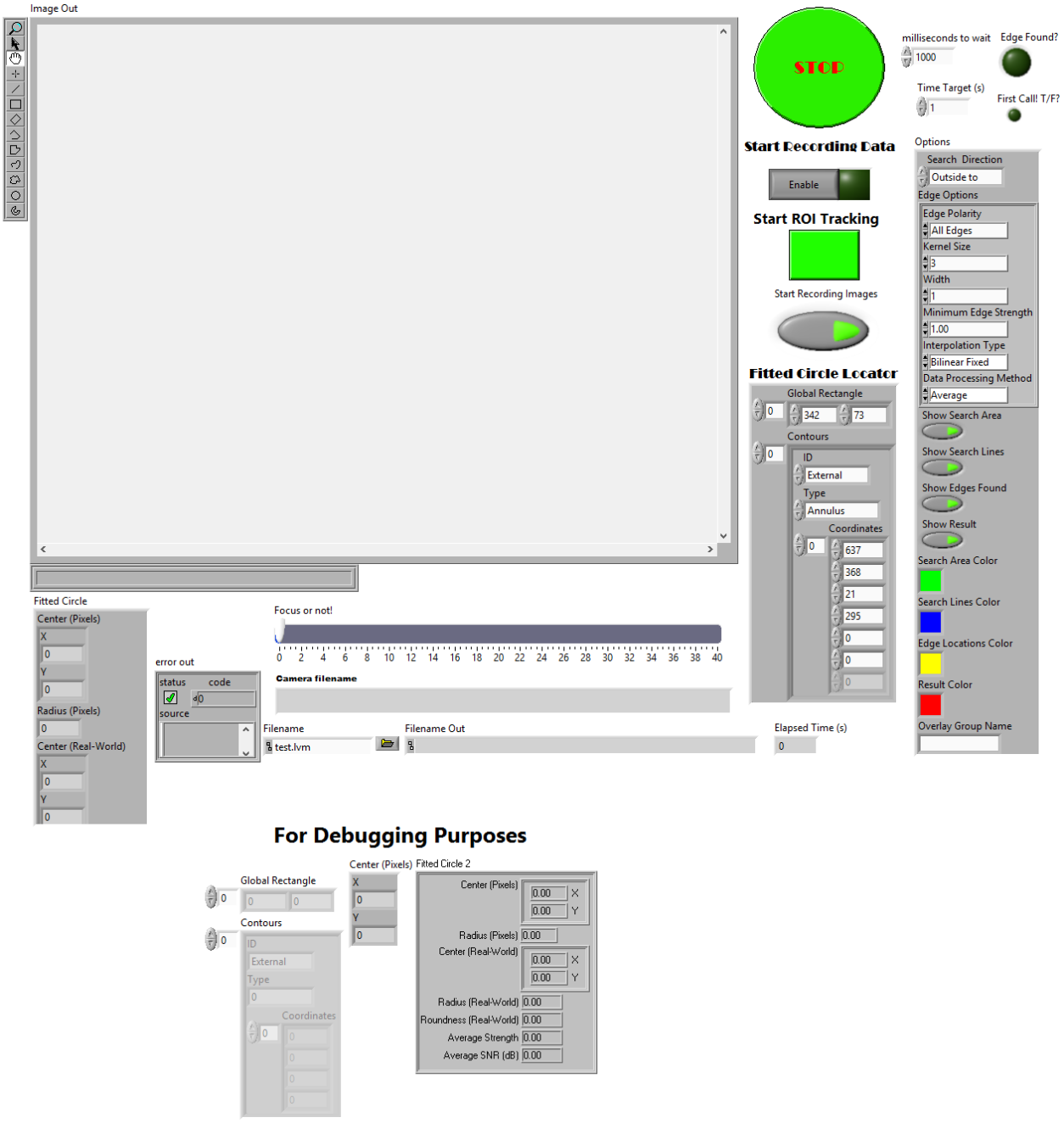

Figure 43: LabVIEW™ interface Front Panel.

Appendix 2

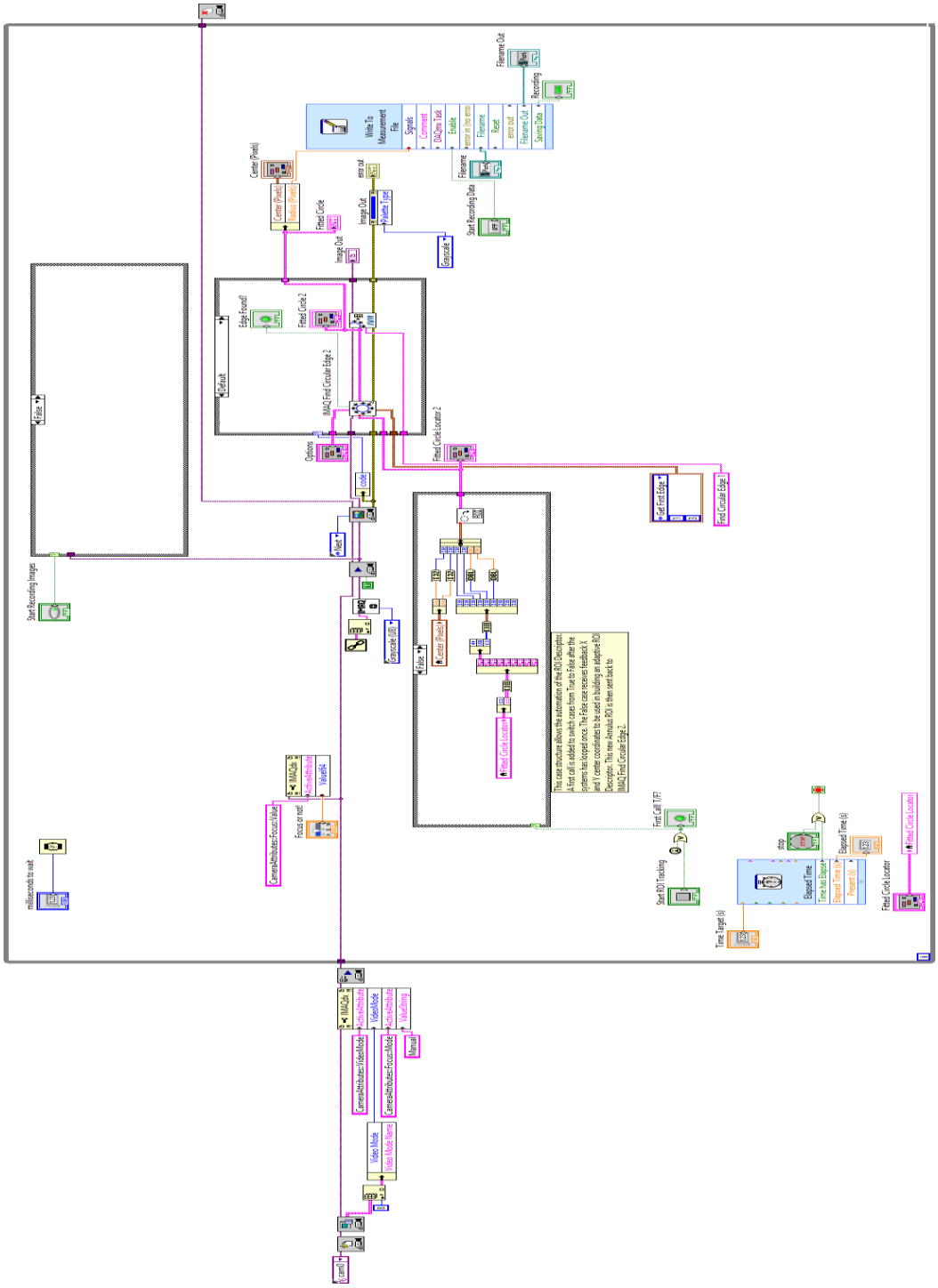

Figure 44: LabVIEW™ block diagram for simple image acquisition code (non binary code).

Appendix 3

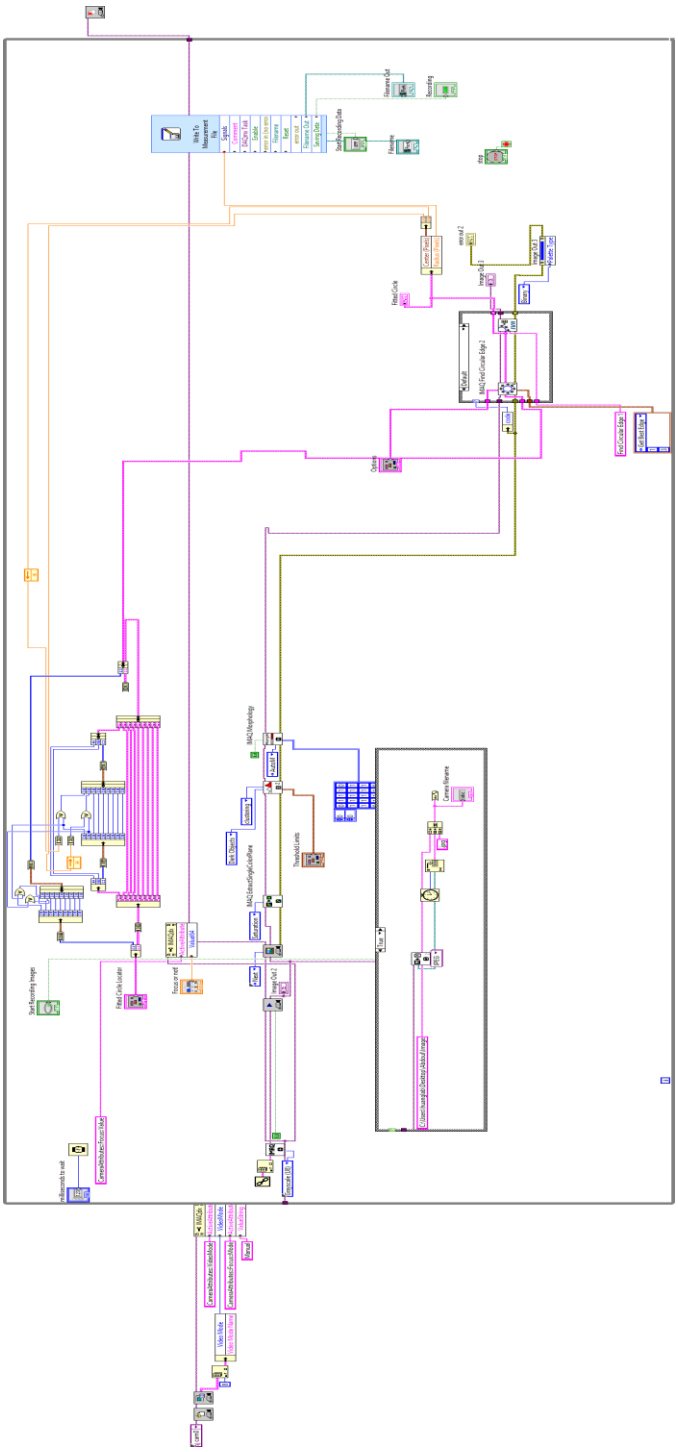

Figure 45: LabVIEW™ block diagram for binary image acquisition.

Appendix 4

```
clear
clc
% This matlab script will plot data obtained from a data acquisition
% set up. The goal is to automate the analysis process to minimize human
% intervention during that process.

% data is the data collected which will be added to the data analysis
% path.

load data1 ; t= data(:,1); Ra=data(:,2);
t1= data1(:,1); Ra1=data1(:,2);

e= length(data);e1= length(data1);



for i=1:e
    r(i)= abs(Ra(1)-Ra(i))/Ra(1); % This is the expansion percent
                                  % as del(D)/D
end
for i=1:e1
     z(i)=abs(Ra1(1)-Ra1(i))/Ra1(1);
end
f=fit(t,r','exp2')
w=fit(t1,z','exp2')
plot(f,t,r,'*');
hold on
plot(w,'g',t1,z,'*')
xlabel('Time(s)')
ylabel('Del(D)/D')
title('50% w/w Cu-PDMS in Toluene')
```

Appendix 5

```
clear
clc
% This matlab script will plot data obtained from a data acquisition
% set up. The goal is to automate the analysis process to minimize human
% intervention during that process.

% data1 is the data collected which will be added to the data analysis
% path.

load data1 ; t= data(:,1); Ra=data(:,2);
t1= data1(:,1); Ra1=data1(:,2);

n=min(length(Ra), length(Ra1));
R=22.3; % Initial sample diameter
for i=1:n
    r(i)= abs(R-Ra(i))/R; % This is the expansion percent
                          % as del(D)/D
end

for i=1:n
     r1(i)=abs(R-Ra1(i))/R;
end

f=fit(t(1:n,:),r','exp2')
fave=fit(t(1:n,:),(r(:,1:n)'+r1')/2,'exp2')
f1=fit(t1(1:n,:),r1','exp2')
figure
plot(fave,t(1:n,:),(r(:,1:n)+r1)/2,'*');
hold on
plot(f,t(1:n,:),r,'*')
plot(f1,'g',t1(1:n,:),r1,'*')

xlabel('Time(s)')
ylabel('Del(D)/D')
title('50% w/w Cu-PDMS in Toluene')
```

Appendix 6:

```
clear
clc
% This matlab script will plot data obtained from a data acquisition
% set up. The goal is to automate the analysis process to minimize human
% intervention
clear
clc
% This matlab script will plot data obtained from a data acquisition
% set up. The goal is to automate the analysis process to minimize human
% intervention during that process.

% data is the data collected which will be added to the data analysis
% path.
format compact
load datall ;

% The following take an average of the two data set collected for the
% same percent copper concentration. Hint the sets of data labeled for
% example "data 121" as the 1st sets of data of 20%CuPDMS.
for i=1:min(length(data321),length(data322))
Ra2(i)=abs(data321(i,2)+data322(i,2))/2;
end
for i=1:min(length(data331),length(data332))
Ra3(i)=abs(data331(i,2)+data332(i,2))/2;
end
for i=1:min(length(data341),length(data342))
Ra4(i)=abs(data341(i,2)+data342(i,2))/2;
end
for i=1:min(length(data351),length(data352))
Ra5(i)=abs(data351(i,2)+data352(i,2))/2;
end
for i=1:min(length(data361),length(data362))
Ra6(i)=abs(data361(i,2)+data362(i,2))/2;
end
for i=1:min(length(data371),length(data372))
Ra7(i)=abs(data371(i,2)+data372(i,2))/2;
end
for i=1:min(length(data381),length(data382))
Ra8(i)=abs(data381(i,2)+data382(i,2))/2;
end
n1=min(length(Ra2),length(Ra3));n2=min(length(Ra4),length(Ra5));
n3=min(length(Ra6),length(Ra7));n13=min(length(data381),length(data382));
n11=min(n1,n2);n12=min(n11,n3); n=min(n12,n13);% Selecting the shortest array.
t=1:.5:n/2+.5;
```

```
R1=22.30; % these are used as base diameter (in pixels) for calculating
        % the expansion.
R2=29.09;
for i=1:n
    r2(i)=abs(R1-Ra2(i))/R1;
end
for i=1:n
    r3(i)=abs(R1-Ra3(i))/R1;
end
for i=1:n
    r4(i)=abs(R2-Ra4(i))/R2;
end
for i=1:n
    r5(i)=abs(R2-Ra5(i))/R2;
end
for i=1:n
    r6(i)=abs(R2-Ra6(i))/R2;
end
for i=1:n
    r7(i)=abs(R2-Ra7(i))/R2;
end
for i=1:n
    r8(i)=abs(R2-Ra8(i))/R2;
end
f2=fit(t',r2','exp2')
f3=fit(t',r3','exp2')
f4=fit(t',r4','exp2')
f5=fit(t',r5','exp2')
f6=fit(t',r6','exp2')
f7=fit(t',r7','exp2')
f8=fit(t',r8','exp2')
figure
plot(f2,'b',t,r2,'c*')
hold on
plot(f3,'k',t,r3,'g*')
plot(f4,t,r4,'y*')
plot(f5,'g',t,r5,'r*')
plot(f6,'y',t,r6,'k*')
plot(f7,'c',t,r7,'m*')
plot(f8,'r',t,r8,'b*')
grid on
axis([0 n/2 0 0.4])
xlabel('Time(seconds)')
ylabel('Del(D)/D')
title('20% - 80% w/Total.w Cu2Oxide-PDMS in Toluene')
legend 20pCu 20pfit 30pCu 30pfit 40pCu 40pfit 50pCu 50pfit 60pCu 60pfit ...
```

```
   70pCu 70pfit 80pCu 80pfit
n during that process.

% data is the data collected which will be added to the data analysis
% path.
format compact
load datall ;

% The following take an average of the two data set collected for the
% same percent copper concentration. Hint the sets of data labeled for
% example "data 121" as the 1st sets of data of 20%CuPDMS.
for i=1:min(length(data321),length(data322))
Ra2(i)=abs(data321(i,2)+data322(i,2))/2;
end
for i=1:min(length(data331),length(data332))
Ra3(i)=abs(data331(i,2)+data332(i,2))/2;
end
for i=1:min(length(data341),length(data342))
Ra4(i)=abs(data341(i,2)+data342(i,2))/2;
end
for i=1:min(length(data351),length(data352))
Ra5(i)=abs(data351(i,2)+data352(i,2))/2;
end
for i=1:min(length(data361),length(data362))
Ra6(i)=abs(data361(i,2)+data362(i,2))/2;
end
for i=1:min(length(data371),length(data372))
Ra7(i)=abs(data371(i,2)+data372(i,2))/2;
end
for i=1:min(length(data381),length(data382))
Ra8(i)=abs(data381(i,2)+data382(i,2))/2;
end
n1=min(length(Ra2),length(Ra3));n2=min(length(Ra4),length(Ra5));
n3=min(length(Ra6),length(Ra7));n13=min(length(data381),length(data382));
n11=min(n1,n2);n12=min(n11,n3); n=min(n12,n13);% Selecting the shortest array.
t=1:.5:n/2+.5;
R1=22.30; % these are used as base diameter (in pixels) for calculating
        % the expansion.
R2=29.09;
for i=1:n
    r2(i)=abs(R1-Ra2(i))/R1;
end
for i=1:n
    r3(i)=abs(R1-Ra3(i))/R1;
end
for i=1:n
```

```
    r4(i)=abs(R2-Ra4(i))/R2;
end
for i=1:n
    r5(i)=abs(R2-Ra5(i))/R2;
end
for i=1:n
    r6(i)=abs(R2-Ra6(i))/R2;
end
for i=1:n
    r7(i)=abs(R2-Ra7(i))/R2;
end
for i=1:n
    r8(i)=abs(R2-Ra8(i))/R2;
end
f2=fit(t',r2','exp2')
f3=fit(t',r3','exp2')
f4=fit(t',r4','exp2')
f5=fit(t',r5','exp2')
f6=fit(t',r6','exp2')
f7=fit(t',r7','exp2')
f8=fit(t',r8','exp2')
figure
plot(f2,'b',t,r2,'c*')
hold on
plot(f3,'k',t,r3,'g*')
plot(f4,t,r4,'y*')
plot(f5,'g',t,r5,'r*')
plot(f6,'y',t,r6,'k*')
plot(f7,'c',t,r7,'m*')
plot(f8,'r',t,r8,'b*')
grid on
axis([0 n/2 0 0.4])
xlabel('Time(seconds)')
ylabel('Del(D)/D')
title('20% - 80% w/Total.w Cu2Oxide-PDMS in Toluene')
legend 20pCu 20pfit 30pCu 30pfit 40pCu 40pfit 50pCu 50pfit 60pCu 60pfit ...
    70pCu 70pfit 80pCu 80pfit
```

Appendix 7

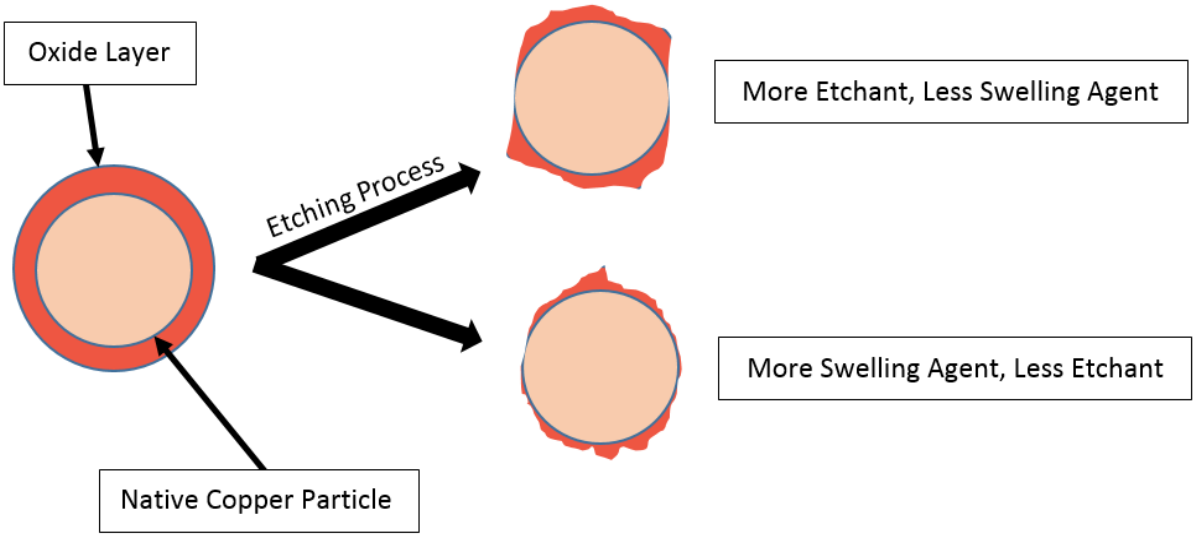

Figure 46: Copper (I) oxide removal effect by varying the etchant percentage in the etching bath.